RESEARCH ARTICLE

WILEY

White matter tract strength correlates with therapy outcome in persistent developmental stuttering

Nicole E. Neef[1,2] 🟢 | Alexandra Korzeczek[2] | Annika Primaßin[2,3] | Alexander Wolff von Gudenberg[4] | Peter Dechent[5] | Christian Heiner Riedel[1] | Walter Paulus[2] | Martin Sommer[2,6,7]

[1]Department of Diagnostic and Interventional Neuroradiology, University Medical Center Göttingen, Göttingen, Germany

[2]Department of Clinical Neurophysiology, University Medical Center Göttingen, Göttingen, Germany

[3]Fachbereich Gesundheit, FH Münster University of Applied Sciences, Münster, Germany

[4]Institut der Kasseler Stottertherapie, Bad Emstal, Germany

[5]Department of Cognitive Neurology, MR Research in Neurosciences, University Medical Center Göttingen, Göttingen, Germany

[6]Department of Neurology, University Medical Center Göttingen, Göttingen, Germany

[7]Department of Geriatrics, University Medical Center Göttingen, Göttingen, Germany

Correspondence
Nicole E. Neef, Department of Diagnostic and Interventional Neuroradiology, University Medical Center, Georg August University, Robert-Koch-Straße 40, 37075 Göttingen, Germany.
Email: nneef@gwdg.de

Funding information
Deutsche Forschungsgemeinschaft, Grant/Award Number: SO 429/4-1

Abstract

Persistent stuttering is a prevalent neurodevelopmental speech disorder, which presents with involuntary speech blocks, sound and syllable repetitions, and sound prolongations. Affected individuals often struggle with negative feelings, elevated anxiety, and low self-esteem. Neuroimaging studies frequently link persistent stuttering with cortical alterations and dysfunctional cortico-basal ganglia-thalamocortical loops; dMRI data also point toward connectivity changes of the superior longitudinal fasciculus (SLF) and the frontal aslant tract (FAT). Both tracts are involved in speech and language functions, and the FAT also supports inhibitory control and conflict monitoring. Whether the two tracts are involved in therapy-associated improvements and how they relate to therapeutic outcomes is currently unknown. Here, we analyzed dMRI data of 22 patients who participated in a fluency-shaping program, 18 patients not participating in therapy, and 27 fluent control participants, measured 1 year apart. We used diffusion tractography to segment the SLF and FAT bilaterally and to quantify their microstructural properties before and after a fluency-shaping program. Participants learned to speak with soft articulation, pitch, and voicing during a 2-week on-site boot camp and computer-assisted biofeedback-based daily training for 1 year. Therapy had no impact on the microstructural properties of the two tracts. Yet, after therapy, stuttering severity correlated positively with left SLF fractional anisotropy, whereas relief from the social–emotional burden to stutter correlated negatively with right FAT fractional anisotropy. Thus, post-treatment, speech motor performance relates to the left dorsal stream, while the experience of the adverse impact of stuttering relates to the structure recently associated with conflict monitoring and action inhibition.

KEYWORDS
diffusion MRI, FAT, neural speech networks, SLF, stuttering intervention, tractography

1 | INTRODUCTION

Enhanced speech fluency is the ultimate goal of behaviorally oriented stuttering treatment and a key to establishing relief from stuttering. Behavioral fluency shaping programs modify speech tempo, prosody, rhythm, voicing, and breathing (Max & Caruso, 1997; Webster, 1974, 1980) and dramatically reduce overt stuttering (Euler, von Gudenberg, Jung, & Neumann, 2009; Frigerio-Domingues et al., 2019; von Gudenberg & Euler, 2000). Fluency shaping programs cause, in addition, a reappraisal of the disorder itself by reducing the covert symptoms of stuttering (Euler et al., 2021; Frigerio-Domingues et al., 2019). The spectrum of such covert components is vast, including struggle behavior, avoiding words or communication, negative feelings toward specific communication situations, and elevated anxiety (Freud & Amir, 2020). However, to date, our knowledge is limited about brain structures and mechanisms that underly fluency shaping-based improvements of stuttering.

Neuroimaging studies report therapy-associated normalizations of the otherwise imbalanced activity of the orbital part of bilateral inferior frontal gyri (Kell et al., 2009; Kell, Neumann, Behrens, von Gudenberg, & Giraud, 2018; Neumann et al., 2018) together with adjusted functional connectivity between the pars opercularis of the inferior frontal gyrus, the articulatory motor cortex, the supplementary motor cortex, The supramarginal gyrus, and the anterior superior temporal gyrus (Kell et al., 2018). The basal ganglia and the cerebellum also show therapy-related changes of activity (Nil, Kroll, & Houle, 2001; Toyomura, Fujii, & Kuriki, 2015) and connectivity (Lu et al., 2012, 2017). Hence, the reorganization of brain function involves large-scale cortical and subcortical networks related to speech processes, auditory-motor coupling, sequential motor planning, and timing.

Only one study investigated therapy-associated white matter changes (Neef et al., 2021). As fluency shaping therapy influences the neural control of the larynx by changing pitch and voicing patterns, this previous study tested the impact of a 1-year intensive fluency shaping on the structural connectivity of cortical representations of the laryngeal motor control. Diffusion tractography-based analyses did not show training-related changes in structural networks underlying voice control. However, several crucial questions remained unanswered. Despite the missing impact on white matter structures of the laryngeal motor networks, it is unclear whether structures involved in speech and language processing, auditory-motor coupling, sequential motor planning, or timing support stuttering remediation. Being implicated in the functional reorganization, neuroplasticity within such structures seems plausible (Kell et al., 2018). Here, we reanalyzed diffusion MRI (dMRI) data from our previous study to probe structural connectivity changes in two major fiber tracts that are required for fluent speech production, that is, the superior longitudinal fasciculus/arcuate fasciculus (SLF/AF) and the frontal aslant tract (FAT).

SLF and AF constitute the fiber tracts that are theoretically conceptualized as the dorsal language pathway (Hickok & Poeppel, 2007; Saur et al., 2008). The SLF III links Brodmann area 44 in the inferior frontal gyrus pars opercularis (IFG) with the supramarginal gyrus in the inferior parietal lobe (Schmahmann & Pandya, 2006). The AF originates in the caudal part of the superior temporal gyrus and superior temporal sulcus and projects to the dorsal part of areas 8, 46, and 6 as

initially proven via autoradiography in macaque brains (Schmahmann & Pandya, 2006). Some previous DTI studies define the AF in agreement with (Catani, Jones, & ffytche, 2005) and differentiate a long segment (AF$_{long}$) the fiber pathway that connects IFG and precentral gyrus with the superior temporal and middle temporal gyrus, and an anterior segment (AF$_{ant}$) that links IFG, middle frontal gyrus and ventral precentral gyrus with the inferior parietal lobule (Catani et al., 2005; Catani & Mesulam, 2008). Ample evidence exists to suggest that the AF contributes to syntactic (Catani & Bambini, 2014; Friederici, Bahlmann, Heim, Schubotz, & Anwander, 2006), phonological processing (Glasser & Rilling, 2008; Sarubbo et al., 2015), and auditory-motor mapping (Elmer et al., 2019). The SLF III on the other hand is involved in fluent speech production (Bonilha et al., 2019). Early diffusion tensor imaging (DTI) studies associated persistent developmental stuttering with a weak left SLF/AF as quantified via an activation likelihood estimation (ALE) meta-analysis across experiments using tract-based spatial statistics (TBSS) (Neef, Anwander, & Friederici, 2015). More recent studies used tractography to investigate white matter microstructure and morphological characteristics of tracts. Available data regarding white matter characteristics of the SLF/AF in persistent developmental stuttering are inconsistent. People who stutter show either smaller tract volumes of the left AF (Kronfeld-Duenias, Amir, Ezrati-Vinacour, Civier, & Ben-Shachar, 2016a) or bilateral AF (Cieslak, Ingham, Ingham, & Grafton, 2015) or no differences (Connally, Ward, Howell, & Watkins, 2014; Kronfeld-Duenias, Civier, Amir, Ezrati-Vinacour, & Ben-Shachar, 2018) when compared with controls. Tract fractional anisotropy (FA) was reduced in the right AF (Kronfeld-Duenias et al., 2016a) or bilaterally in SLF/AF (Connally et al., 2014; Neef et al., 2017) or similar (Kronfeld-Duenias et al., 2018). The few available tractography studies on stuttering used different diffusion models, tractography algorithms, seed and tract definitions, tract metrics, and strategies to correct for multiple comparisons, providing, altogether, a rather vague understanding of the condition (Kronfeld-Duenias et al., 2018). Given the vital contribution of the dorsal stream to speech and language processing, we selected the SLF to test therapy-associated changes.

The FATs connect the inferior frontal gyri with the presupplementary and supplementary motor area (Catani et al., 2012; de Schotten, Dell'Acqua, Valabregue, & Catani, 2012). The left FAT contributes to speech and language functions, the right FAT is involved in inhibitory control, and both FAT pathways may underly sequential motor planning (Dick, Garic, Graziano, & Tremblay, 2018). Notably, right frontal white matter structures harbor characteristic neuroanatomical correlates of stuttering, including an increased white matter volume in the inferior frontal gyrus, the precentral gyrus in the vicinity of the face and mouth representation, and the anterior middle frontal gyrus (Jäncke, Hänggi, & Steinmetz, 2004). Furthermore, persistent developmental stuttering has been associated with altered diffusion properties of the left and right FAT with an increased mean diffusivity (MD), axial diffusivity (AD), and radial diffusivity (RD) in persons who stutter (PWS) compared to controls (Kronfeld-Duenias, Amir, Ezrati-Vinacour, Civier, & Ben-Shachar, 2016b). Furthermore, MD within the left FAT correlated negatively with speech rate (Kronfeld-Duenias et al., 2016b) and the connection probability of the

right FAT correlated positively with stuttering severity (Neef et al., 2017). Intraoperative axonal electrical stimulation of the FAT induced stuttering symptoms in tumor patients with no preoperative stuttering (Kemerdere et al., 2016). These previous findings underline the critical role of the FAT in fluent speech production, and we therefore also selected the FAT to test therapy-associated changes.

Here, we analyzed dMRI data from a more extensive study on evaluating the long-term effects of an intensive fluency shaping program on white-matter integrity and task-related brain activity (Primaßin, 2019). In earlier analyses of these data, we used probabilistic diffusion tracking with seeds in the laryngeal motor representations (LMC) and quantified connection probability of the structural LMC networks, including the somatosensory cortex, inferior parietal cortex, inferior frontal gyrus, superior temporal gyrus, SMA, caudate nucleus, putamen, and globus pallidus (Neef et al., 2021). This previous study showed no therapy-associated connectivity changes of the LMC networks. However, SLF and FAT were not tested in these previous analyses. To answer the question of whether these two tracts undergo neuroplastic structural changes, we used the Automated Fiber Quantification (AFQ) software and studied diffusion properties along these two major speech tracts. Furthermore, we tested the relationship between tract composition and behavioral outcome.

2 | METHODS

Data were collected in the context of a larger project on the evaluation of the long-term effects of an intensive stuttering intervention on brain structure and function (Primaßin, 2019). In a previous publication of the dMRI data of this cohort, probabilistic diffusion tractography was used to compare structural networks of the dorsal laryngeal motor cortex and the ventral laryngeal motor cortex (Neef et al., 2021).

2.1 | Participants

We invited patients who were about to begin with intervention at the Kassel Stuttering Therapy (KST) to participate in the current MRI study (PWS+). Fluent controls (HC) were invited via advertisements at the homepage of the Department of Clinical Neurophysiology and at notice boards of the university campus and clinic. Stuttering controls (PWS−) were recruited via announcements at stuttering self-help groups and at the 2016 annual congress of the German stuttering self-help group association (BVSS). PWS− did not participate in any stuttering intervention during the entire study period.

All participants were monolingual native speakers of German. We included 22 people who stutter and participated in a 1-year fluency shaping program (PWS+, two females, mean age = 26.6 years, range 14–57 years, SD = 11.7 years), 18 people who stutter not participating in therapy (PWS−, two females, mean age = 34.8 years, range 26–47 years, SD = 7.0 years) and 27 typically fluent healthy controls (HC, 4 females, mean age = 24.8 years, range 14–52 years, SD = 7.4 years). Groups were matched for sex, χ^2 (2) = .39, p = .821,

and handedness, χ^2 (2) = .05, p = .975. PWS+ and HC had a similar age (W = 228, p = .695, r = −.06), PWS− were older compared to PWS+ (W = 77, p < .001, r = −.47), and compared to HC (W = 59, p < .001, r = −.35). PWS+ and PWS− were matched for age at stuttering onset, W = 190, p = .815, r = −.04, and their last therapy dated back for a similar amount of years, $t(30)$ = 1.17, p = .249. Inter-session intervals ranged between 10 and 15 months and were similar for the three groups, χ^2 (2) = .85, p = .652. Demographic data are given in Table 1. Participants reported normal hearing, had no history of hearing, speech, language, or neurological deficits apart from stuttering in the PWS groups, drug abuse, or medications that act on the central nervous system.

According to the Declaration of Helsinki, the ethical review board of the University Medical Center Göttingen, Georg August University Göttingen, Germany, approved the study, and all participants gave their written informed consent. In addition, we obtained informed consent from parents or legal guardians of participants younger than 18 years.

We registered the study in January 2016 at the Study Center of the University Medical Center Göttingen (registration number 01703). Registration is accessible via sz-umg.registrierung@med.uni-goettingen.de.

2.2 | Behavioral assessment

Per session, we assessed participants' speech with the Stuttering Severity Instrument, SSI-4 (Riley, 2009). Participants were video-recorded and scored offline by two certified speech–language pathologists (one of them was A.P., who was not blinded to the treatment groups). The frequency and duration of stuttered syllables and physical concomitants were scored in reading and conversation samples, with each sample containing 488–500 syllables. As described in earlier studies (Korzeczek et al., 2021; Primaßin, 2019), the inter-rater reliability was quantified for the speech samples of nine participants, three randomly chosen from each group. With .96, KALPHA of the SSI-4 total score indicated a good to excellent consensus between raters. Pre-intervention, PWS+ had a median total SSI-4 score of 25 with an interquartile range of 15–31. According to the SSI-4 severity levels, five of the 22 PWS+ were categorized as very mild, five as mild, six as moderate, three as severe, two as very severe, and one with an SSI-4 total score of 7 was not classified. At session one, PWS− had a median total SSI-4 score of 14 with an interquartile range of 7–21. Eight of the 18 PWS− were categorized as very mild, two as mild, one as moderate, one as severe, one as very severe, and five with SSI-4 scores between four and seven were not classified. Before therapy, stuttering severity was more severe in PWS+ as compared to PWS− (Figure 1a,e).

We used the Overall Assessment of the Speaker's Experience of Stuttering (OASES) to evaluate intervention-associated reappraisal of stuttering, as its score strongly correlates with a person's capacity to use coping mechanisms with stressors and challenges, that is, resilience (Freud & Amir, 2020). The OASES (Yaruss & Quesal, 2006, 2014) captures the covert manifestation of stuttering, behavioral and emotional reactions, struggle and avoidance, and its implications on communication and quality of life. Participants completed the German

TABLE 1 Demographic information of the individual participants

Group	Sex	Age (years)	Education	LI	Interval (months)	Onset (years)	Last (years)	SSI T1	SSI T2	OASES T1	OASES T2
PWS+	m	40	2	82	10	6	29	28	17	3.17	1.79
PWS+	m	23	2	−100	10	6	1	16	4	3.18	1.53
PWS+	m	29	3	82	12	2	19	23	15	2.07	1.91
PWS+	m	28	3	100	12	4	16	27	5	3.11	1.66
PWS+	m	24	2	100	12	5	7	38	30	3.23	2.13
PWS+	m	30	2	80	11	9	Nan	13	6	2.52	2.05
PWS+	m	16	2	−100	12	4	1	22	9	*2.65	*1.51
PWS+	m	19	3	100	12	5	Nan	13	8	2.96	2.13
PWS+	m	21	4	67	12	3	4	19	7	3.00	1.83
PWS+	m	27	5	100	11	3	17	10	5	2.18	1.63
PWS+	f	18	3	100	12	2	2	18	5	2.33	2.06
PWS+	m	15	1	82	12	3	5	39	37	*2.69	*2.33
PWS+	m	28	2	100	12	2	1	30	17	2.74	2.48
PWS+	f	16	1	100	11	13	2	7	5	*2.51	*1.41
PWS+	m	19	3	82	11	4	2	24	2	3.18	2.08
PWS+	m	14	1	100	12	2	7	31	11	*2.87	*2.24
PWS+	m	16	1	82	10	4	8	26	15	*3.21	*1.65
PWS+	m	54	6	100	13	12	25	32	12	2.99	1.81
PWS+	m	21	2	100	11	4	12	28	1	3.10	1.22
PWS+	m	32	6	82	12	2	3	32	9	3.19	3.02
PWS+	m	57	2	100	14	6	1	33	22	3.64	2.15
PWS+	m	17	2	67	10	4	Nan	11	9	*3.59	*1.89
PWS−	m	38	2	100	11	2.5	29	28	26	2.99	2.72
PWS−	m	28	6	100	10	2	2	7	8	1.38	1.27
PWS−	m	28	6	100	12	6	8	5	8	1.58	1.67
PWS−	m	26	3	100	10	2	4	15	13	1.30	1.27
PWS−	m	34	6	64	11	2	15	4	4	1.89	1.87
PWS−	m	28	3	54	10	6	13	22	15	2.04	1.80
PWS−	f	28	6	67	15	3	8	14	12	2.21	2.25
PWS−	m	36	6	82	15	3	2	16	18	2.13	2.45
PWS−	m	47	6	82	12	2	16	42	44	2.25	2.17
PWS−	m	43	6	100	11	3	10	7	10	2.08	1.91
PWS−	m	34	3	82	12	2	Nan	20	22	1.73	1.71
PWS−	m	30	6	100	11	10	11	10	4	2.16	2.20
PWS−	m	46	7	100	12	14	14	11	11	1.86	1.92
PWS−	m	44	7	100	11	2	15	32	35	2.46	2.28
PWS−	m	35	2	−20	12	5	Nan	5	3	1.83	1.69
PWS−	m	33	6	67	11	7	Nan	14	16	2.44	2.13
PWS−	f	27	3	100	11	10	3	15	16	2.10	2.12
PWS−	m	43	5	67	11	8	31	11	10	1.80	1.98
HC	m	35	2	82	12			2	0		
HC	m	24	5	−67	11			0	0		
HC	f	20	3	100	11			0	0		
HC	m	28	3	100	14			0	0		
HC	m	20	3	100	13			5	0		

TABLE 1 (Continued)

Group	Sex	Age (years)	Education	LI	Interval (months)	Onset (years)	Last (years)	SSI T1	SSI T2	OASES T1	OASES T2
HC	m	28	6	100	12			1	0		
HC	m	27	3	60	12			0	0		
HC	m	24	5	67	12			0	0		
HC	m	30	6	67	12			5	0		
HC	m	21	3	82	11			4	2		
HC	m	22	5	67	11			0	0		
HC	f	17	2	100	12			4	2		
HC	m	31	6	100	11			4	4		
HC	f	17	1	−67	11			0	0		
HC	f	23	5	−54	11			0	0		
HC	m	27	4	43	11			5	3		
HC	m	52	3	100	10			0	0		
HC	m	27	5	100	11			0	0		
HC	m	14	1	100	11			0	0		
HC	m	19	2	100	12			4	5		
HC	m	17	2	82	11			7	9		
HC	m	18	2	100	11			8	9		
HC	m	28	3	100	11			0	0		
HC	m	27	3	82	11			0	0		
HC	m	25	5	100	11			0	3		
HC	m	27	4	100	11			0	0		
HC	m	23	3	100	11			2	0		

Abbreviations: *OASES-T, Assessment of the Speaker's Experience of Stuttering for Teenagers; f, female; HC, healthy controls; Interval, time span between session one and session two; Last, years since last therapy; LI, laterality index of Edinburgh Handedness Inventory; m, male; OASES, Assessment of the Speaker's Experience of Stuttering (Yaruss & Quesal, 2014); Onset, age at stuttering onset; PWS−, stuttering patients without stuttering intervention; PWS+, stuttering patients with stuttering intervention; Scale of Education−graduation after 1 = still attending school, 2 = school, 3 = high school, 4 = <2 years college, 5 = 2 years college, 6 = 4 years college, and 7 = postgraduate; SSI, Stuttering Severity Index (Riley, 2009); T1, session one−prior to intervention; T2, session two−after intervention.

version of the OASES questionnaire (Yaruss & Quesal, 2014) in both sessions. According to the OASES severity levels, none of the PWS+ was categorized as mild, two as mild to moderate, nine as moderate, 11 as moderate to severe, and none as severe. Two of the 18 PWS− were categorized as mild, 12 as mild to moderate, four as moderate, and none as moderate to severe or severe. Before therapy, the OASES scores were higher in PWS+ than PWS−, indicating an increased stuttering-related stress level in PWS+ (Figure 1b,f).

2.3 | Intensive stuttering intervention and follow-up care

PWS+ took part in the Kasseler Stottertherapie (Euler et al., 2009), an intensive fluency shaping program that incorporates computer-assisted biofeedback during a 2-week on-site and 1-year follow-up treatment. This approach was first introduced with Webster's precision fluency shaping program (Max & Caruso, 1997; Webster, 1974, 1980). The overarching aim is to train to speak slowly with gentle onsets of phonation, light articulatory contacts, and soft voicing of plosives. The Kassel Stuttering Therapy (KST) version of the program uses computer-assisted speech training, group therapy, and assisted real-life training with a training load of at least 8 h per day and 7 d per week. Computer-assisted training at home consisted of the daily biofeedback-assisted practice of the new speech patterns. A compliance agreement with the health insurance enforced participants to practice home at the computer for at least 1,980 min in the first 6 months and 990 min in the following months to reimburse therapy costs. In addition, PWS+ participated in two refresher courses at the therapy center, 1 month and 10 months after enrolment.

2.4 | MRI acquisition protocol

MRI data were acquired in a 3 Tesla Siemens Magnetom Tim Trio scanner (Erlangen, Germany) using an eight-channel, phased-array head coil at the University Medical Center Göttingen, Germany. Sagittal T1-weighted structural data were acquired with a 3D turbo fast
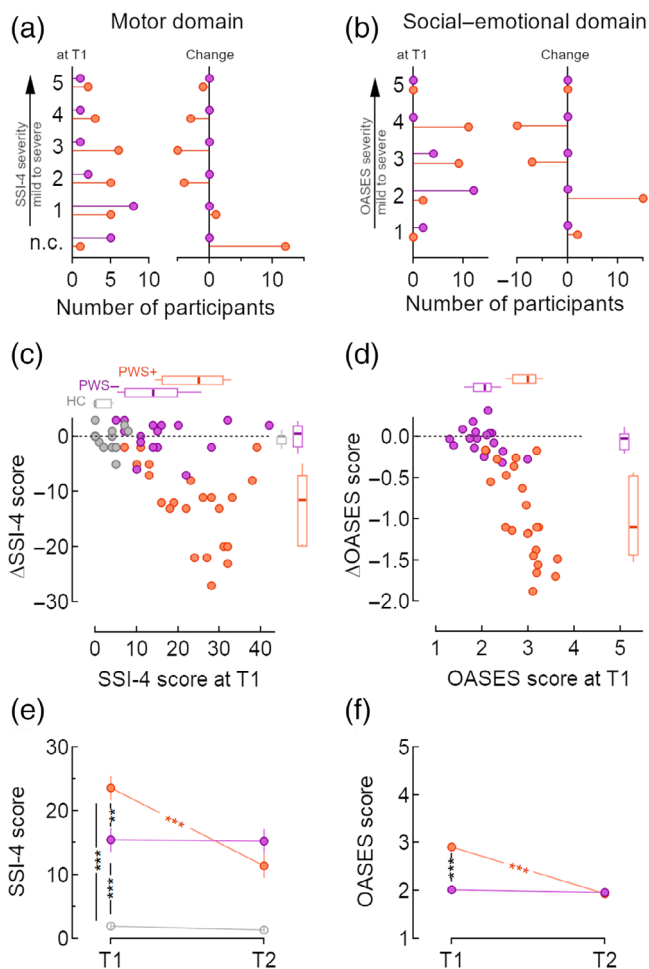
FIGURE 1 Therapy reduced stuttering severity. Stick charts display the number of participants for each severity level (1—mild to 5—severe, n.c. not classified) at T1 and the change in the number of participants for the SSI-4 total score (a) and the OASES total score (b). Scatterplots display the SSI-4 total score (c) and the OASES total scores at T1 (d) against the magnitude of its change. Boxplots indicate the group median with the interquartile range and whiskers of one *SD*. Group × Time interactions are displayed with the group means ± SEM at T1 and T2, separated for the SSI-4 scores [$\chi^2(10, N = 67) = 62.13$, $p < .001$; $Z = −10.08$, ∗∗∗adjusted $p < .001$] with an effect size of $r = .77$ (e), and the OASES scores [$\chi^2(8, N = 40) = 33.35$, $p < .001$; $Z = −7.21$, ∗∗∗adjusted $p < .001$] with an effect size of $r = .75$ (f). Fluent controls (HC, gray) and persons who stuttered and did not participate in therapy (PWS−, purple) showed no changes across time. In contrast, persons who stutter and participate in therapy (PWS+, orange) showed a reduction of stuttering symptoms in the motor domain and a reduction of the negative impact of stuttering on their daily lives (social–emotional domain). Wilcoxen test significant at ∗∗∗$p < .001$, ∗∗$p = .01$

low angle shot (FLASH) sequence (TR = 2,250 ms, TE = 3.26 ms, TI = 900 ms, flip angle = 9°, 256 mm FoV, 7/8 Fourier phase encoding) as whole-brain anatomical reference data at a spatial resolution of $1 \times 1 \times 1$ mm³ voxel size (256×256 matrix). Diffusion-weighted MRI was collected with a spin-echo EPI sequence (TR = 10,100 ms, TE = 93 ms, parallel acquisition factor 2, 6/8

Fourier phase encoding, 243 mm FoV, acquisition matrix: 128×128, 74 slices, voxel size $1.9 \times 1.9 \times 1.9$ mm³) acquiring 64 image volumes with diffusion weighting along 64 diffusion directions (b = 1,000 s/mm²) and one reference image without diffusion weighting. Participants lay supine in the scanner, wore headphones for noise protection and MR-compatible LCD goggles (VisuaStim XGA, Resonance Technology Inc., Northridge, CA).

2.5 | MRI data processing and analyses

Diffusion data were preprocessed with tools from the FMRIB Software Library (FSL 6.0 on a Linux machine with Ubuntu LTS 18.04, http://www.fmrbi.ox.ac.uk/fsl/). Fiber tracking was carried out on aligned, distortion corrected, concatenated datasets that were collected across session one and session two for each subject to ensure that estimates of diffusivity and diffusion anisotropy across sessions were mapped to the same anatomical location for each subject. White matter tracts were identified with the Automated Fiber Quantification software implemented in python (pyAFQ, https://github.com/yeatmanlab/pyAFQ; Yeatman, Dougherty, Myall, Wandell, & Feldman, 2012). Within pyAFQ individual b0 images were aligned with the native anatomy via an affine registration and warped to the FSL_HCP1065_FA_1mm template via a nonlinear registration. Inverted warp maps were used to register waypoint masks and exclusion masks with individual b0 images. A whole-brain tractogram was generated in the native space of each participant with a deterministic tracking algorithm with a fourth-order Runge–Kutta path integration method (1 mm fixed step size, eight seed points per voxel, FA threshold .2 and 30°, minimum streamline length set to 10 mm). A three-step procedure implemented in pyAFQ (https://github.com/yeatmanlab/pyAFQ) was used to segment the superior longitudinal fasciculus (SLF) and the frontal aslant tract (FAT). First, the whole brain tractography was filtered with tract-specific probability maps with a probability of .25. The probability maps for the left and right SLF were provided with pyAFQ software. The maps for the FAT were taken from FMRIB Software Library (FSL 6.0), providing the population percentage tract atlases of the left and right FAT, respectively (Warrington et al., 2020). In the next step, filtered tractograms were additionally filtered with waypoint and exclusion masks. A sagittal mask through the corpus callosum was used for every tract segmentation to exclude streamlines crossing hemispheres. In addition, the waypoint and exclusion masks for the left and right SLF were provided with pyAFQ software. The waypoint masks for the left and right FAT were taken from https://github.com/yeatmanlab/AFQ/tree/master/aslant/ROIs (Kronfeld-Duenias et al., 2016b). Additionally, native anatomy was skull stripped, tissue segmented, and anatomically labeled with FreeSurfer 6.0 (https://surfer.nmr.mgh.harvard.edu/). This enabled anatomical endpoint filtering, ensuring that segmented streamlines terminate in defined cortical regions. Visual inspection of the tracts and manual cleaning was performed via TrackVis 0.6.1 (http://trackvis.org/). Tracts with less than 10 streamlines were excluded from further analyses (Table S1). Finally, we fitted the

diffusion kurtosis model, implemented in DIPY (https://dipy.org/; Garyfallidis et al., 2014), to the diffusion data separately for each session and projected the FA, MD, RD, and AD onto the segmented fiber tracts generated by pyAFQ. Selected tracts were sampled into 100 evenly spaced nodes, spanning the two termination points. To determine changes in diffusion properties, we calculated the difference curve between session one and session two and averaged the values of the inner 60 nodes. This procedure was adopted from a report of rapid white matter changes after an intensive reading intervention (Huber, Donnelly, Rokem, & Yeatman, 2018).

2.6 | Statistics

We used RStudio Version 1.4.1717, R version 4.1.0, packages nlme_3.1-152, FSA_0.8.32, and gmodels_2.18.1 to calculate statistics.

2.6.1 | Statistical analyses of behavioral data

We tested the changes in behavior with mixed-effects models. We set two group contrasts, one to compare PWS+ with PWS− and HC, and one to compare PWS− with HC. Because the OASES is only applicable in PWS, the OASES models included only one group contrast to compare PWS+ with PWS−. In addition, we set the time contrast to compare T2 with T1. With the lme() function, we specified the baseline model that included only the dependent variable as a fixed-effects predictor and participant and time as repeated-measures predictors. We used the maximum likelihood method to estimate the model. To see the overall effect of each main effect and interaction, we added predictors age, group, time, and Group × Time one at a time.

2.6.2 | Statistical analyses of the averaged middle 60% of each tract

To test changes of white matter properties (FA, MD, RD, and AD) over time, we averaged the middle 60% of each tract to create a single estimate of diffusion properties for each subject and tract (Huber et al., 2018). Mean tract values were entered into linear mixed-effects models with participant and time as repeated-measures predictors. Predictors age, group, time, and Group × Time were added one at a time. Models were calculated for each tract and diffusion property.

Furthermore, to model the effect of the stuttering trait, we pooled diffusion properties at T1 across both stuttering groups and fed the middle 60% mean values into linear fixed-effects models. In these trait models, the group contrast was set to compare PWS and HC. Predictors age, group, and Age × Group were added one at a time.

All models were compared with the ANOVA() function. We quantified the effect size r for the highest order interactions. In case

interactions were not significant, we quantified the effect size of significant lower-order contrasts.

2.6.3 | Statistical analyses at each point along the tract

For all participants, unpaired t-tests were performed at each of the 100 points along the tracts to test differences between PWS and HC at T1 for FA, MD, RD, and AD. To correct for the 100-fold comparison, we performed Monte-Carlo simulations to determine which cluster length can be expected to appear randomly, given the .05 alpha level of the permutation test. For PWS+, we performed unpaired t tests at each of the 100 points along the tracts to test changes of diffusion properties when comparing T2 with T1, and determined cluster significance with Monte-Carlo simulations. Furthermore, we calculated pointwise Pearson correlations to test brain-behavior relationships for the dMRI metrics along the four tracts. Specifically, we tested the correlation between diffusion metrics (FA, MD, RD, AD) and stuttering severity (SSI total score, OASES total score) at T1 and at T2. We used bootstrapping with a boot size of 100,000 to determine significant correlations at $p < .005$ with a cluster-size significance at $p < .01$. Pointwise statistics were calculated with MATLAB (R2018b).

2.6.4 | Statistical tests on the influence of age

Because pointwise statistics yielded significant clusters in some portions of the tracts, we performed additional analyses to explore the relationship between brain, behavior, and age. Therefore, we extracted diffusion property values from the significant clusters and performed bivariate Pearson correlations between FA, age, and SSI-score for the cluster in the left SLF, and between FA, age, and OASES in the right FAT (Figure S1). Furthermore, we calculated partial correlations between FA and behavior accounting for the influence of age, because partial correlations are a way to separate the influences of multiple co-variables on an outcome. Finally, we calculated fixed-effects models to test the influence of age on mean FA and mean AD of significant clusters of the pointwise trait analyses. We added predictors group and age one at a time. For all GLM analyses, alpha level was set to .05 and adjusted with the Holm method.

3 | RESULTS

3.1 | Intervention improved speech fluency and stuttering reappraisal in PWS+

Therapy changed the SSI-4 severity levels in PWS+. Specifically, 13 out of 22 PWS+ changed from very severe, severe, moderate, or mild, to the level "very mild" or lower, that is, below SSI-4 severity categories (Figure 1a). In contrast, no participant of the PWS− group

changed the SSI-4 severity level. SSI-4 total scores at T1 and the change in SSI-4 are shown for each participant (Figure 1c). The mixed model analysis revealed a Group × Time interaction and main effects of group and time (Table S3, Figure 1e). SSI-4 total scores decreased in PWS+ from T1, $M_{T1} = 23.6$, $SD = 9.2$, to T2, $M_{T2} = 11.4$, $SD = 9.0$, but remained unchanged in PWS−, $M_{T1} = 15.4$, $M_{T2} = 15.3$, $SD = 10.8$, and HC, $M_{T1} = 1.9$, $SD = 2.5$, $M_{T2} = 1.4$, $SD = 2.6$.

Therapy also reduced the negative social–emotional impact of stuttering. Specifically, 17 PWS+ who were categorized by OASES as moderate-to-severe or moderate reached the two lowest categories mild-to-moderate and mild after therapy (Figure 1b). None of the PWS− changed the OASES severity level. OASES total score at T1 and the change in OASES are shown for each participant (Figure 1d), and the mixed model analysis revealed a Group × Time interaction and main effects of group and time (Table S4, Figure 1f). In PWS+, the OASES score decreased from T1, $M_{T1} = 2.9$, $SD = .4$, to T2,

$M_{T2} = 1.9$, $SD = .4$. In contrast, PWS− showed no decrease, $M_{T1} = 2.0$, SD = .4, $M_{T2} = 2.0$, SD = .4.

3.2 | No intervention-related changes of SLF and FAT diffusion properties

Therapy had no effect on SLF or FAT tract profiles (Figure 2a,b). Delta FA and delta MD are shown for each participant for the middle 60% of each tract (Figure 2c,d), and mixed model analyses on mean values of middle 60% FA, MD, RD, or AD revealed no significant effects or interactions, except one (Tables S5–S8). Across groups, left SLF mean FA decreased from T1, $M_{T1} = .524$, $SD = .04$, to T2, $M_{T2} = .516$, $SD = .04$ as indicated by the significant effect of time $[\chi^2(8, N = 64) = 9.67, p = .002; Z = -3.05$, mixed model adjusted $p = .014]$ with an effect size of $r = .35$.
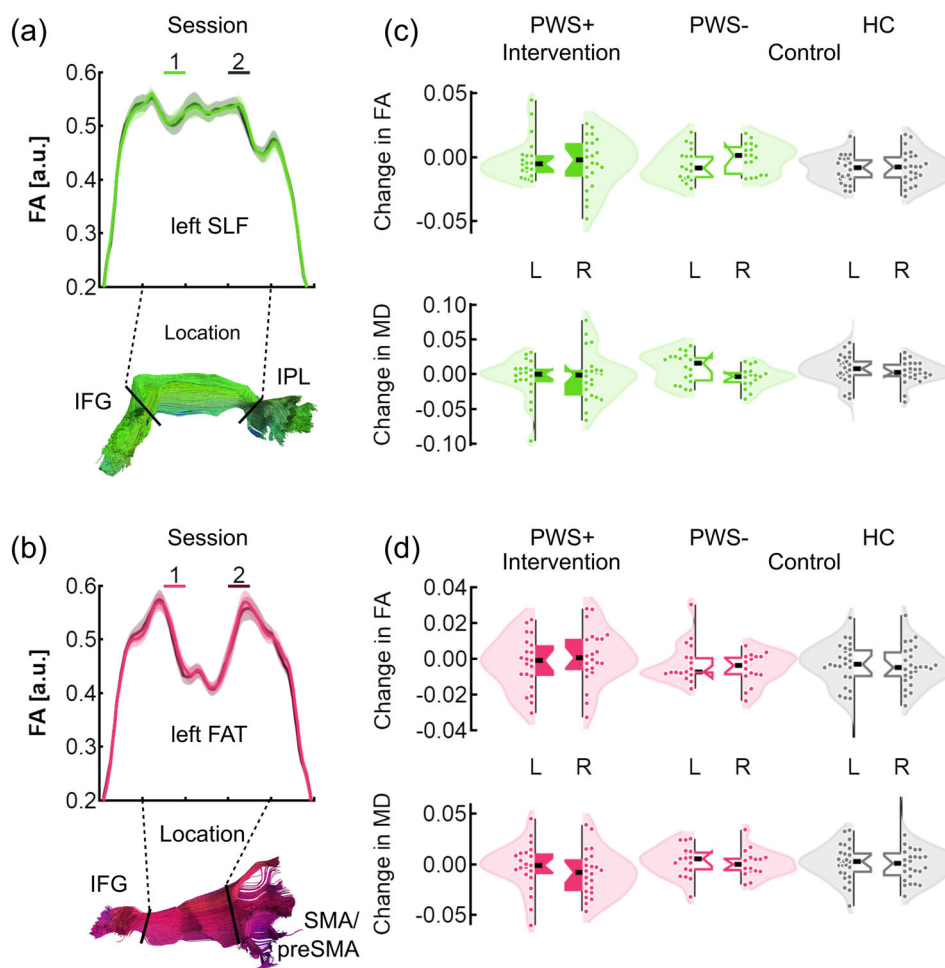
FIGURE 2 No intervention-related white matter changes in SLF or FAT. Fractional anisotropy, FA, was mapped onto 100 evenly spaced points connecting cortical speech regions. Each curve represents the group average FA across participants of the intervention group (PWS+, $n = 22$) for the white matter of (a) the left superior longitudinal fasciculus (SLF, green) and (b) the left frontal aslant tract (FAT, red). Pale colors show pre-intervention FA (Session 1), and dark colors show FA after 11 months of intervention (Session 2). The shaded areas give the standard error of the mean. Each tract was clipped before analysis as indicated by the black boundary lines in corresponding tract renderings. (c,d) Only the middle 60% of each tract was considered in the analyses of FA and mean diffusivity, MD. Raincloud plots illustrate the magnitude of change observed relative to Session 1 for the left (L) and right (R) tract for the intervention group (filled boxes) and the two control groups (stuttering without intervention, PWS−; and fluent speakers without intervention, HC; unfilled boxes). Individual data points, distributions, median FA with the interquartile range, and whiskers from minimum to maximum are displayed

In PWS+, further permutation tests for each of the 100 points along the tracts were not significant when comparing FA, MD, RD, or AD between T1 and T2.

3.3 | Persistent stuttering alters SLF and FAT diffusion properties

Fixed effect model analyses of diffusion properties before intervention revealed no effects of group when testing mean FA (Figure 3), MD, RD, or AD of the middle 60% of the tracts, but there was an effect of age on MD of the left SLF [χ^2(4, N = 64) = 6.04, p = .014; Z = −2.74, adjusted p = .018] with an effect size of r = .32, and an effect of age on RD of the left SLF [χ^2(4, N = 64) = 3.37, p = .066; Z = −2.57, adjusted p = .030] with an effect size of r = .31 (Tables S9–S11).

Further permutation tests for each of the 100 points along with the tracts revealed for PWS a significantly reduced FA in the anterior and middle portion of the right SLF (Figure 3), significantly increased AD in the middle portion of the left FAT, and significantly decreased AD in the anterior portion of the left FAT (Figure 3). There was no significant influence of age on the group differences in the right SLF and the middle portion of the left FAT, but the group difference in the anterior portion of the right FAT decreased significantly with increasing age [χ^2(4, N = 64) = 3.37, p = .066; Z = −2.57, adjusted p = .030] with an effect size of r = .31 (Table S13, Figure S3).

3.4 | Posttreatment, white matter integrity of SLF and FAT was related stuttering severity

In PWS+, the group that participated in therapy, left SLF FA and SSI-4 total scores correlated negatively in the posterior portion of the tract at T2 (Figure 4a,c). Thus, after the intervention, mild stuttering was related to higher FA values, while severe stuttering was related to lower FA values in the left SLF. At session one, correlations in the same SLF region did not survive correction for multiple comparisons (Figure 4a,c). We calculated a z-score of the difference between the correlation coefficients. With a difference score of z = 1.79 and a two-tailed p = .073, the correlations between FA at session two and SSI-4 tended to be stronger than the correlation between FA at session one and SSI-4. No other correlation between SSI-4 and white matter characteristics reached statistical significance. To further investigate the influence of age on this brain-behavior relationship, we calculated bivariate and partial correlations. In the particular region of the left SLF, there were no significant correlations between age and FA (Figure S1a, top left), between age and SSI-4 (Figure S1a, top right), or between age and the change in SSI-4 (Figure S2a). Furthermore, age did not explain the correlation between posttherapy SSI-4 scores and left SLF FA (Figure S1a, bottom right). The significant partial correlation at T2 demonstrated this after accounting for age, r (17) = −.71, p = .0007.

Finally, in PWS+, the psychosocial impact of stuttering, as measured with the OASES, was positively correlated with the middle portion of the right FAT at T2 (Figure 4b,d). Thus, after the intervention, mild suffering from stuttering was related to lower FA values, while severe suffering from stuttering was related to higher FA values in the right FAT. With a difference score of z = −2.89 and a two-tailed p = .004, the correlation between FA at session two and OASES was significantly stronger than the correlation between FA at session one and OASES. No other correlation between OASES and white matter characteristics reached statistical significance. To further investigate the influence of age on this brain-behavior relationship, we calculated bivariate and partial correlations. There were significant negative correlations between age and FA in the right FAT at T1 [r(20) = −.65, p = .001] and at T2 [r(20) = −.59, p = .004, Figure S1b top left].

FIGURE 3 Pre-intervention tract FA. Each curve represents the group average FA and SEM (transparent area) for pooled people who stutter (PWS, n = 40) and healthy fluent controls (HC, n = 27) at T1. Permutation tests at each of the 100 points along the tracts revealed group differences at p < .05 (cluster-size p = .0125 in red, uncorrected p < .05 in black), with neighboring points (uncorrected p < .1 in gray) for FA, MD, RD, and AD. Raincloud plots display individual data points, distributions, median with the interquartile range and whiskers from minimum to maximum of the middle 60%
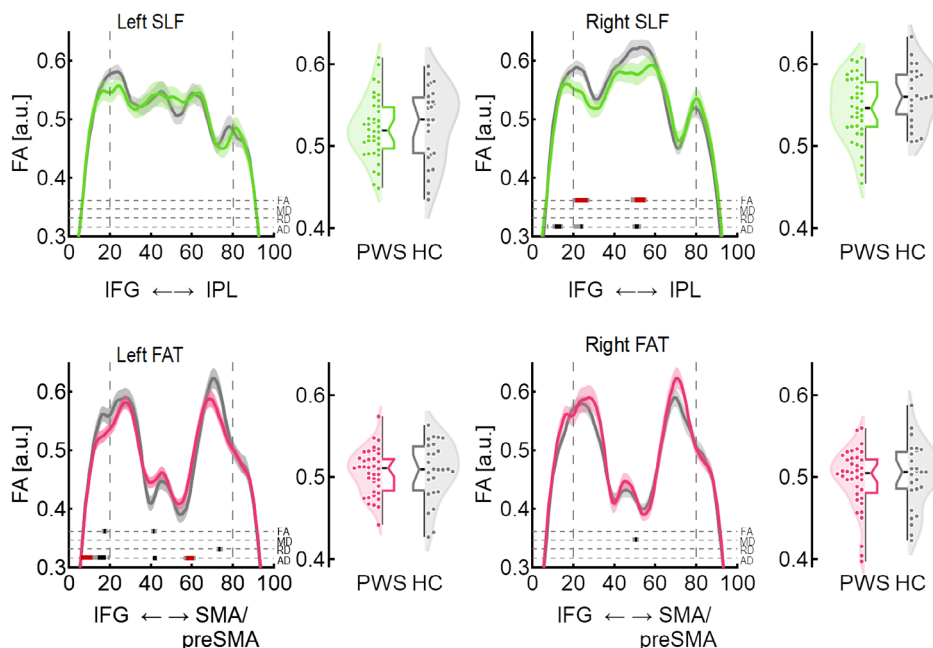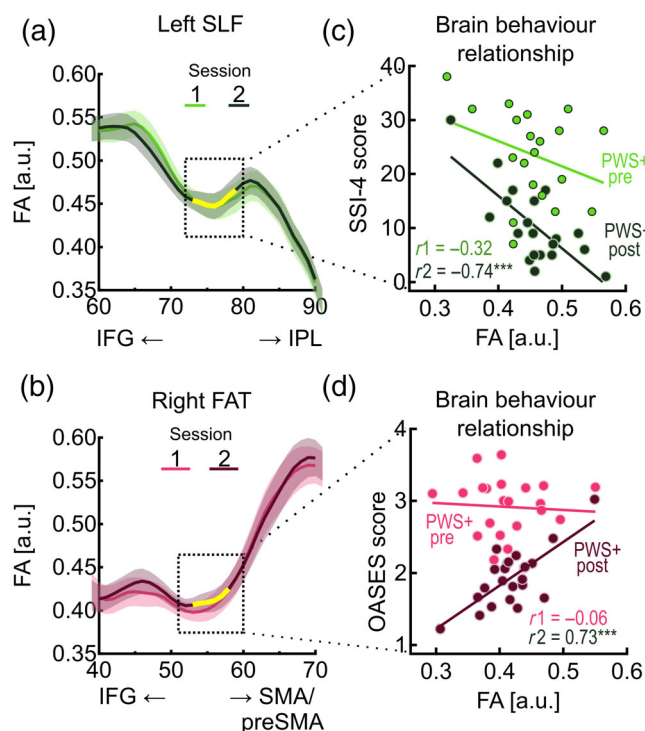
FIGURE 4 Brain behavior relationship changed with intervention. Each curve represents the group average FA across participants of the intervention group (PWS+) from the posterior part of the left superior longitudinal fasciculus (SLF, a), and from the medium part of the right frontal aslant tract (FAT, b). Pale colors show pre-intervention FA (Session 1), and dark colors show post-intervention FA (Session 2). Shaded areas represent one standard error of the mean. (c) Stuttering severity (SSI-4 scores) is plotted against FA values averaged across tract points 73–81 framed with a dotted square in a. The Pearson correlation was significant at ***$p < .001$. Bootstrapping with a boot size of 100,000 revealed significant pointwise correlations at $p < .005$ with a cluster-size significance at $p < .01$ highlighted with yellow in a. (d) Experience of stuttering (OASES scores) is plotted against FA values averaged across tract points 52–61 framed with a dotted square in b. The Pearson correlation was significant at ***$p < .001$. Bootstrapping with a boot size of 100,000 revealed significant pointwise correlations at $p < .005$ with a cluster-size significance at $p < .02$ highlighted with yellow in b

These negative correlations indicate that younger participants had a higher FA, whereas older participants had a lower FA in the particular region of the right FAT that correlated with the OASES score. Furthermore, age and change in OASES score showed a significant negative correlation [$r(20) = -.57$, $p = .006$, Figure S2a], indicating that older participants showed a more substantial reduction of the negative psychosocial impact of stuttering. At the same time, older participants had lower FA values, which were correlated with low OASES scores posttherapy. These two observations are consistent with each other. However, age was not significantly correlated with OASES scores at T1 or T2 (Figure S1b, top right) and, most importantly, age did not explain the correlation between posttherapy OASES scores and right FAT FA values (Figure S1b, bottom right). The significant partial correlation at T2 demonstrated this after accounting for age, $r(19) = .68$, $p = .0008$.

4 | DISCUSSION

This study tested whether stuttering therapy induces speech tract neuroplasticity. One year of fluency-shaping training ameliorated stuttering, but white matter diffusion properties of SLF and FAT remained unchanged. Pre-intervention, PWS had a reduced FA in the anterior and middle portion of the right SLF, and a reduced AD in the anterior portion but an increased AD in the middle portion of the left FAT. Most importantly, therapy-associated relief from stuttering correlated with FA in the left SLF and the right FAT. Specifically, higher FA in the left SLF was related to lower stuttering severity scores following therapy. So, after therapy, those with higher FA in this tract showed the lowest SSI-4 scores. Thus, a stronger SLF relates to a better speech motor performance: lower frequency of stuttered syllables, shorter durations of stuttering events, and fewer physical concomitants. Furthermore, lower FA in the right FAT was related to a lower score on the OASES, the measure of the psychosocial impact of stuttering. So, after therapy, those with lower FA in the right FAT showed the lowest OASES scores. Thus, a weaker right FAT was related to a less negatively perceived experience and attitude toward stuttering posttherapy. Because the correlations emerged even though tract compositions remained stable, we suggest that the composition of the two speech tracts might support the behavioral outcome of the intensive fluency shaping training.

4.1 | No effect of successful therapy on white matter microstructure

The present finding of unchanged white matter microstructure in SLF and FAT is consistent with our previous study. An earlier analysis of different white matter structures in the same data set likewise revealed no therapy-associated structural connectivity changes (Neef et al., 2021). Specifically, fluency shaping practice did not modify the structural network connectivity of the dorsal and ventral laryngeal motor cortices. On the other hand, practicing fluency shaping for 1 year increased functional connectivity within the sensorimotor network. Specifically, therapy increased resting-state connectivity between the left dorsal laryngeal motor cortex and the left IFG and between the left dorsal laryngeal motor cortex and the right pSTG (Korzeczek et al., 2021). Because these two connections showed no pathological findings before therapy, the functional neuroplasticity indicated learning-related changes rather than a normalization of altered network dynamics. Furthermore, our observations indicate that therapy changed network dynamics while speech-related cortico-cortical fiber bundles remained unchanged.

Only one other previous study exists with DTI data in a cohort of PWS who participated in stuttering therapy. However, this previous study reported no pre-/post-intervention comparisons of the dMRI measures (Kell et al., 2009). In contrast, patients with other speech and language disorders showed training-induced white matter changes. For example, intensive intonation-based speech therapy reduced FA in the white matter underlying the right IFG, pSTG, and

posterior cingulum in patients with nonfluent aphasia (Wan, Zheng, Marchina, Norton, & Schlaug, 2014). In addition, intensive voice treatment increased FA in white matter tracts of the speech production network in children with cerebral palsy and motor speech disorders (Reed, Cummine, Bakhtiari, Fox, & Boliek, 2017). The latter finding is consistent with reports in other domains. Training- and therapy-induced increases in FA and decreases in MD have been reported for motor (Drijkoningen et al., 2015; Lehmann, Villringer, & Taubert, 2020; Reid, Sale, Cunnington, Mattingley, & Rose, 2017), sensory (Maeda et al., 2017), sensorimotor (Scholz, Klein, Behrens, & Johansen-Berg, 2009), and cognitive interventions (Huber et al., 2018; Metzler-Baddeley et al., 2017).

Here, we used an analysis approach that has been first described for intensive reading skills training (Huber et al., 2018). Huber and colleagues observed increased mean FA and decreased mean MD in the reading network of grade-school-aged children. Compared to the current study, participants of the reading training were young, and measurements took place in a time window when developmental changes of white matter properties are still rapid (Yeatman, Wandell, & Mezer, 2014). Thus, significant white matter changes might have evolved from the structured intensive learning program because of neuroplasticity dynamics that are natural at such a young age. Here, one possible explanation of why the current longitudinal study could not find white matter changes in principal tracts of the speech network might be that our participants were older and varied broadly in age (range 14–57 years). Compared to other association tracts, the SLF has a prolonged maturation. At age 14, FA still slowly increases, reaching the maturation-related peak between age 28 and 35 (Lebel et al., 2012) before aging-related decline kicks in (Voineskos et al., 2012). In addition, the SLF consists of three branches that vary for developmental and aging processes (Amemiya, Naito, & Takemura, 2021). Thus, different neurobiological mechanisms shape white matter properties with complex temporal dynamics during development and aging, which possibly renders the detection of training-induced changes difficult.

Because SLF displays developmental FA changes throughout the age range of our cohorts, there is a possibility that the observed decrease of FA across all groups might be explained by the previously observed developmental trajectory. We explored this possibility by plotting FA changes against age (Figure S4). The Pearson correlation between these variables was significant with $r = -.32$, $p = .011$. Almost all older participants (>35 years) showed a decrease in FA. In contrast, younger participants showed on average no change in FA. The large variability of FA change that overlays this effect of age is probably a combination of true intraindividual variation and the limited precision of dMRI. The observed FA decrease in the age group above approximately 35 years resembles the pattern described for white matter maturation and aging in the SLF (Lebel et al., 2012). Thus, the effect of time across groups for left SLF FA might be partly explained by the influence of development and aging on white matter diffusion properties, even though the time between measurements was only 1 year.

Another reasonable explanation for the lack of white matter plasticity could be the extended training period, which caused a long gap between measurements. Here, fluency-shaping was trained daily for 1 year, and white matter changes were assessed only after this 1 year. Previous training studies tested changes in white matter metrics after shorter training periods. For example, the study with intensive intonation-based speech treatment in patients with aphasia lasted for 15 weeks (Wan et al., 2014). The study with the training of vocal loudness lasted for 4 weeks and included a maintenance period of another 12 weeks (Reed et al., 2017). Learning-associated white matter changes have been reported even after as little as two times 45 min of practice in a balancing task (Taubert et al., 2010). The few studies that quantified the time course of learning-associated structural changes reported complex dynamics, strongly varying between individuals and brain structures. This included slowly manifesting changes and transient processes (Quallo et al., 2009; Taubert et al., 2010; Taubert, Villringer, & Ragert, 2012). Since our study included no interleaved MRI sessions, we cannot exclude transient white matter changes that might have occurred during the intervention.

Furthermore, the training studies mentioned above observed white matter changes that are sometimes counterintuitive. Some studies reported a decrease in FA (Scholz et al., 2009; Taubert et al., 2010; Wan et al., 2014), whereas others showed the likelier increases in FA (Reed et al., 2017; Scholz et al., 2009). Diffusion metrics are influenced by various macro-, meso-, and microstructural properties such as fiber number, myelination and diameter, and fiber fanning and crossing, only to name a few. Consequently, FA reductions might result from structural changes that are hard to disentangle (Zatorre, Fields, & Johansen-Berg, 2012). In summary, although learning is typically associated with FA increases and MD decreases, the absence of such changes does not necessarily indicate unchanged FAT and SLF tracts because dMRI measures cannot directly inform us about the underlying fiber properties and related neurobiological processes that mediate learning-associated changes (Zatorre et al., 2012).

Finally, the restriction of the current analyses to four tracts limits the current conclusions. We focussed on the SLF and the FAT because of their prominent role in stuttering pathology and speech motor control. However, other fiber bundles are also associated with stuttering persistency and pathology. For an overview, see Kronfeld-Duenias et al. (2018). Accordingly, an exhaustive analysis of white matter structures may include the inferior longitudinal fasciculus (Kronfeld-Duenias et al., 2018), cingulum (Kronfeld-Duenias et al., 2018), and transcallosal (Chow & Chang, 2017; Garnett et al., 2018; Kronfeld-Duenias et al., 2018), cerebellar (Connally et al., 2014; Johnson, Liu, Waller, & Chang, in press; Jossinger et al., 2021a), and cortico-spinal and cortico-bulbar fiber bundles (Connally et al., 2014). In case such extended analyses would link therapy with white matter plasticity, it may furthermore help to include additional control tracts with no expected changes to determine the specificity of the therapy. Because of the restricted analyses, we cannot exclude neuroplastic changes in other white matter structures.

4.2 | Tract geometry interferes with diffusion properties along tracts

In the current study, FA heavily varies along the tracts (Figures 2–4), a pattern that is also visible in other studies (e.g., Johnson et al., in press; Perron, Theaud, Descoteaux, & Tremblay, 2021). This variance is deterministic since it occurs in the individual tracts with a similar trajectory. Still, it is reasonable to assume that this variance impacts averaged diffusion metrics. Let us shortly elaborate on the concept of diffusion tensor imaging. Numerous studies link diffusion metrics to specific microstructural phenomena or structures. It is assumed that FA represents the overall directionality of water diffusion in a voxel. AD informs about the diffusivity parallel to the principal axis of the tensor, which was often interpreted as diffusivity along axonal fibers. RD informs about the diffusivity in the two minor axes, which is often interpreted as diffusivity perpendicular to the axonal fibers, and MD represents the mean of the three primary axes of the tensor (Bihan et al., 2001). However, while the corpus callosum provides a suitably simple fiber geometry to link differences in DTI metrics to microstructural differences, such as the link between myelination and RD (Song et al., 2005), most brain regions have complex fiber geometries making it notoriously hard to disentangle specific microstructural conditions or changes (Jones et al., 2013; Mazerolle et al., 2021). The multiple minima and maxima along the FA curves of both tracts (Figures 2–4) are most likely attributed to tract portions with a complex fiber geometry (fiber inflow and outflow, curving, or fanning). Hence, plotted curves do not represent a pure measure of the FA along with a particular fiber bundle, but the variance in FA along the tract most likely indicates varying bundle geometries. This variance might interfere with the actual diffusion metric when averaging the values along a tract. Pointwise analyses along tracts are a possible strategy to account for differences in fiber geometries. Such analyses might bear the problem that neighboring data points are not independent given the spatial resolution of dMRI data. A projection of diffusion metrics to 100 points along a tract likely induces different degrees of data extrapolation depending on the actual length of the tract. This further complicates correction for multiple comparisons, especially when statistical testing was performed at individual points along a segmented fiber tract.

To summarize, statistical analyses on the averaged values of diffusivity metrics across data points along segmented fiber tracts might be affected by varying fiber tract geometries. In contrast, statistics on individual values along a fiber tract might be inflated due to an anatomically implausible upsampling. Hence, both approaches bear disadvantages that complicate a straightforward interpretation of findings.

4.3 | The SLFs implication in stuttering and stuttering therapy

For the SLF, group comparisons of diffusion metrics prior to treatment showed similar tract profiles for averaged FA, MD, RD, and AD. In contrast, pointwise analyses located lower right SLF FA in anterior and middle tract portions of PWS compared to fluent controls. This finding is not new but received less attention in earlier studies. For example, in adults who stutter, bilateral FA reductions were found via TBSS (Cai et al., 2014; Cieslak et al., 2015; Neef et al., 2017) and fiber tracking analyses (Connally et al., 2014; Kronfeld-Duenias et al., 2016a). Also, children who persist in stuttering have been reported to show a lower FA growth rate in the right dorsal tract (Chow & Chang, 2017). However, other studies found a restriction of FA reductions to the left dorsal pathway (Chang, Horwitz, Ostuni, Reynolds, & Ludlow, 2011; Jossinger et al., 2021b) or no group differences at all (Koenraads et al., 2020; Kronfeld-Duenias et al., 2018; Misaghi, Zhang, Gracco, Nil, & Beal, 2018). Anomalies in the white matter connections of sensory-to-articulatory cortices are commonly seen as the neural deficit that causes an insufficient sensorimotor integration and learning in stuttering (Hickok, Houde, & Rong, 2011; Kell et al., 2018; Kim & Max, 2021; Watkins, Smith, Davis, & Howell, 2008).

The inconsistent findings complicate the view on the neurobiological underpinnings of stuttering, an issue that has long been recognized in the literature (Cai et al., 2014; Cieslak et al., 2015; Kronfeld-Duenias et al., 2018). For example, Kronfeld-Duenias et al. (2018) relate these inconsistencies to sample-specific characteristics such as individual differences in personal traits and compensatory mechanisms. Other possible reasons might be moderate sample sizes (Chang et al., 2011; Cieslak et al., 2015; Jossinger et al., 2021b; Misaghi et al., 2018), differences in data curation or analysis approach as discussed in the previous section.

Strikingly, posttreatment left SLF FA was related to stuttering severity after therapy. So, although left SLF FA was not reduced in PWS compared to controls, those PWS+ who had lower left SLF FA values and thus a weaker SLF, showed less success in improving their speech fluency, whereas those PWS+ who had the highest FA and thus the strongest SLF showed a more successful implementation of fluency-shaping. This relationship is in line with the widely accepted view that the left SLF is implicated in stuttering (Chang, Garnett, Etchell, & Chow, 2019; Neef et al., 2015; Watkins, Chesters, & Connally, 2016). In general, the SLF III is postulated to mediate the conversion of auditory input into phonological and articulatory forms supported by verbal working memory areas of the SMG. Lesion-symptom mapping studies support this concept because SLF III lesions disrupt speech repetition, as evident in patients with conduction aphasia or apraxia of speech (Baboyan et al., 2021; Sarubbo et al., 2015). Furthermore, a vital auditory-to-motor mapping is essential to facilitate feedforward and feedback control during speaking (Guenther & Hickok, 2015), particularly when learning and using modified speech and voicing patterns (Darainy, Vahdat, & Ostry, 2019; Korzeczek et al., 2021). Accordingly, our finding likely indicates the supportive function of the left SLF in speech-related sensory-motor mapping and learning. During the intervention, participants learned to speak slowly with gentle onsets of phonation, light articulatory contacts, and soft voicing of plosives. The successful implementation of this speaking behavior resulted in improved fluency. Our finding suggests that the integrity of the SLF is associated with the capacity to

learn, implement and internalize this modified speaking and voicing pattern.

4.4 | The FATs implication in stuttering and stuttering therapy

Like SLF, the FAT showed no group differences when comparing averaged diffusion metrics prior to treatment. However, pointwise analyses revealed an altered AD in the anterior and middle segment of PWS' left FAT, indicating compromised structural connectivity between left IFG and preSMA/SMA. Only few other fiber tracking studies investigated diffusion metrics of the FAT in stuttering. One study observed increased MD, AD, and RD for bilateral FAT tracts, including a cluster of pointwise group differences for MD in the left FAT close to the preSMA/SMA (Kronfeld-Duenias et al., 2016b). In addition, this study reported a correlation between left FAT MD and speech rate. PWS with the highest MD had the slowest speech rates, and PWS with the lowest MD had the fastest. Another study included a small group of 6- to 12-year-old children who stutter and observed increased FA and AD of the right FAT (Misaghi et al., 2018).

Furthermore, a longitudinal study with 35 children who stutter, reported a decreased FA growth rate near a right prefrontal junction of white matter tracts. The observed cluster likely included voxels of the FAT (Chow & Chang, 2017). When discussing their finding, Chow and Chang emphasized the limitations of DTI tractography techniques and inherent difficulties in confidently separating affected tracts in this prefrontal region. Finally, a fiber tracking study in a population-based cohort from the Netherlands with 8- to 12-year-old children suggested that the reduced MD in bilateral FAT parallels the finding of reduced FA in bilateral SLF because of the substantial overlap of these two tracts (Koenraads et al., 2020). Indeed, both tracts originate from the IFG and are hard to disentangle at their origin. Here, the cluster of reduced AD/FA was located in the lateral ventral portion of the left FAT adjacent to gray matter voxels of the IFG and thus proximal to other anatomical connections of the IFG.

Strong support for the implication of the FAT in stuttering comes from a combined TMS-EEG study. Combining the two time-sensitive techniques provided intriguing clues for compromised left FAT connectivity. While recording EEG activity at rest (Busan et al., 2019) stimulated the SMA with single TMS pulses. In PWS, TMS induced an abnormally reduced activity in bilateral SMA, left ventral premotor cortex expanding to the IFG, and right parietal regions. The first part of such TMS-evoked EEG signals indicates the excitability of the stimulated site, and the spatiotemporal distribution corresponds to the spread of activation (Hallett et al., 2017). The finding in PWS implies a sluggish initiation of SMA activity and a compromised spreading activation toward the left premotor cortex and IFG. The reduced activity of the IFG could result from a weak response of the SMA to the TMS pulse. However, weakened structural connectivity via the left FAT could further impede the spread of activation from the SMA toward the IFG.

The left FAT is linked to speech fluency as a disruption of the left FAT induces verbal dysfluency as observed in patients with chronic post-stroke aphasia (Halai, Woollams, & Ralph, 2017) and primary progressive aphasia (Catani et al., 2013). Further evidence comes from intraoperative axonal electrical stimulation of the left FAT. Stimulation immediately affected speech fluency, elicited part-word repetitions, prolongations, or speech blocks during a picture-naming task (Kemerdere et al., 2016). However, disturbed verbal fluency can originate from language deficits (compromised lexical access and retrieval) or motor deficits (faulty speech motor program activation and initiation; Matias-Guiu et al., 2022). Be that as it may, a probabilistic fiber tracking study provided the ultimate test to disentangle language and motor components. Prelingually deaf adults who primarily communicate via sign language showed a dramatically low connection probability of the left IFG with the left preSMA/SMA, while left IFG connections via SLF/AF are intact (Finkl et al., 2019). Because deaf signers possess a developed language system but hardly produce speech sounds, this dissociation indicates a dedicated role of the left FAT in the externalization of speech.

To sum up, few existing studies link stuttering to compromised white matter connections between inferior and superior frontal speech regions. Our finding of altered left FAT white matter properties might be related to the compromised capacity of the left FAT to mediate the activation and initiation of speech motor programs.

Finally, the current study found that the post-treatment right FAT FA was related to the psychosocial impact of stuttering after therapy. Specifically, PWS+ with low FA values in the right frontal aslant tract scored low, while PWS+ with high FA values scored high in the OASES after training. A low OASES score reflects little struggle behavior, rare avoidance behavior, and marginal negative feelings toward specific communication situations or anxiety, which indicates a low negative appraisal of stuttering. Conversely, high OASES scores indicate pronounced negative appraisal of stuttering. We showed that fluency-shaping promoted the adaptation to stuttering-related negative stressors and thus strengthened psychological resilience and coping. Individuals with the lowest FA values in the middle segment of the right FAT (posttreatment) showed the lowest adverse impact of stuttering on their lives after therapy.

The FAT subserves seemingly disparate functions and has been hypothesized to change in response to clinical intervention for stuttering (Dick et al., 2018). More and more studies link the right FAT with executive functions. Executive functions subsume a set of cognitive control processes that regulate thoughts and behavior (Miyake & Friedman, 2012) via inhibitory control, cognitive flexibility, working memory and context monitoring, and attentional processing. For example, a case study with a patient with a low-grade glioma in the right frontal lobe demonstrated that intraoperative electrical stimulation of the FAT interferes with the performance in a Stroop-task (a measure of inhibition) and digit span tasks (a measure of working memory; Rutten et al., 2021). Furthermore, a retrospective dMRI study with 72 neuropsychologically characterized patients related tumors near the right FAT to poorer capacity to shift attention and poor letter fluency, a task that relies on the capacity to initiate,

monitor, and inhibit responses (Landers, Meesters, van Zandvoort, de Baene, & Rutten, 2021).

The FAT connects cortical regions on posterior-to-anterior axes with posterior sites related to motor and action and anterior sites related to cognition and emotion (Eickhoff et al., 2011; Hartwigsen, Neef, Camilleri, Margulies, & Eickhoff, 2019). It is tempting to speculate that this gradual functional organization is also reflected in the interplay between preSMA/SMA and IFG when resolving conflicts between competing actions, thoughts, and emotions (Garic, Broce, Graziano, Mattfeld, & Dick, 2019). This speculation ties in with the view that preSMA/SMA and IFG are part of the domain-general control network (Erika-Florence, Leech, & Hampshire, 2014) and contribute to cognitive control. To the best of our knowledge, there is no study showing a link between the right FAT and emotional regulation, cognitive appraisal, or the support of coping behavior with external or internal stressors. However, dealing with one's thoughts and emotions while producing fluent speech and monitoring the correct technique requires cognitive control and heavily addressed working memory, attentional, and inhibitory control. Behavioral experiments demonstrated altered response inhibition in adults and children who stutter (Eggers, Nil, & den BRHV, 2013; Markett et al., 2016). Moreover, slower response inhibition in PWS is linked to higher OASES scores, indicating a relationship between the adverse impact of stuttering with motor inhibition (Treleaven & Coalson, 2020). Therefore, we suggest that the right FAT FA might reflect the integrity of the connection between the posterior IFG and the preSMA/SMA, and stronger connectivity might be related to a burden to successfully address the domain-general control network.

This proposal remains speculative and awaits deeper investigation. Moreover, it is important to differentiate action inhibition as a component of executive control from the physiological inhibition of neurons that is mediated via the cortico-basal ganglia-thalamo-cortical loops (Hannah & Aron, 2021). Indeed, the cortico-basal ganglia-thalamo-cortical loops are also implicated in stuttering (Chang & Guenther, 2020; Cler, Krishnan, Papp, Wiltshire, & Chesters, 2021; Giraud et al., 2008), and in particular, the inhibitory indirect pathway and the inhibitory hyperdirect pathway might be causally involved (Metzger et al., 2018; Neef et al., 2016, 2017). However, the detailed interplay between action inhibition and neural circuits that convey neural inhibition remains to be studied.

Here again, it is important to discuss the relationship between age and diffusion properties of the FAT. Older PWS+ participants had lower FA in the related region of the right FAT. Such a negative correlation between FA and age is neurobiologically plausible, as it was previously reported in numerous population studies across the life span (e.g., Beck et al., 2021; Sullivan & Pfefferbaum, 2006) and in middle and older-aged humans (e.g., Cox et al., 2016; Tseng et al., 2021). However, age was not significantly correlated with OASES scores at T1 or T2 (Figure S1b top right), and, most importantly, age did not explain the correlation between post-therapy OASES scores and right FAT FA (Figure S1b, bottom right). Therefore, even though low FA was linked to low OASES posttreatment and old age was linked to low OASES posttreatment, age did not explain variance in OASES posttreatment. Accordingly, present correlations support our suggestion that a weak left FAT assisted therapeutic benefit in the social–emotional domain.

4.5 | Limitations

The study was not a controlled randomized clinical trial. Furthermore, participants in the stuttering control group were younger and scored lower in SSI-4 and OASES.

A study-specific limitation that might explain inconsistencies of SLF findings relates to the age of the participants. Ten out of 40 PWS were older than 35 years (25%), whereas one out of 27 HC was older than 35 years (3%). More importantly, 16 PWS were younger than 28 years (40%), whereas 20 HC were younger than 28 years (74%). Thus, a larger proportion of HC participants were at an age when FA is still increasing in the SLF (Lebel et al., 2012), which might have biased HCs group average toward lower FA values. This logic stimulates a follow-up question. If maturation and aging processes mask a potential trait effect, why is there a group difference in the right SLF? Here again, a possible explanation might be that the SLF consists of three functionally segregated branches. In particular, SLF FA is a diffusion metric with different aging dynamics (Amemiya et al., 2021) and lateralization (Amemiya et al., 2021; Gallardo, Wassermann, & Anwander, 2020). However, tract segmentation as implemented in pyAFQ does not differentiate between subsegments of the SLF but determines the structure as a whole. To conclude, age might be the primary confounding variable in the present analysis of trait effects. Therefore, we find it crucial to emphasize that our findings might not generalize beyond the study sample. This limitation mainly impacts between-subjects analyses. Within-subjects analyses on therapy-induced changes are less likely affected.

To date, the SSI-4 is a standard tool to access stuttering severity in clinical and scientific settings. Certainly, stuttering as a condition is versatile and difficult to quantify and frequency-based measures such as SSI-4 and "percent stuttered syllables" only reflect the presence of disfluencies as evident to an external observer and fail to capture the level of effort and control applied by the speaker. Therefore, one could argue that stuttering frequency may not be the appropriate measure to capture treatment-induced changes in brain-behavior relationships. A measure that more directly reflects the level of effort and automaticity might be useful and possibly more sensitive in this context.

It is furthermore crucial to note the known limitations of longitudinal diffusion tensor imaging measurements. Already minor differences in the preprocessing can significantly affect test–retest reliability and thus influence the power to detect neuroplastic changes (Madhyastha et al., 2014). To ensure reliability, we followed the approach by Yeatman (Huber et al., 2018; Yeatman et al., 2012) and carried out fiber tracking on aligned, distortion corrected, concatenated datasets that were collected across session one and session two for each subject to ensure that estimates of diffusivity and diffusion anisotropy across sessions were mapped to the very same anatomical location for each subject.

We used pyAFQ to test therapy-associated white matter property changes in SLF and FAT. DTI analysis methods cover a broad spectrum, and study questions and hypotheses dictate the choice of the computational model to best answer the question. VBM and TBSS help to spot altered white matter regions or time-related changes. However, and despite numerous caveats, today's standard step into studying tract affiliation and particularly tract-specific diffusion characteristics is fiber tracking. The AFQ software is continuously advancing and the version we used already combined probabilistic fiber tracking, constraint by anatomical plausibility, that is, standard tract probability masks, and anatomically plausible termination masks. The current study is the first to test white matter diffusion characteristics of two major speech tracts in the context of intensive stuttering therapy and did not find therapy-associated white matter changes. This is somewhat disappointing and might, among other factors, be caused by choice of tracts, the choice of analysis, the choice of dMRI protocol, or the choice of time of the postintervention dMRI session or simply because intervention did not change white matter diffusion characteristics.

Replication studies will be crucial given the heterogeneous picture that emerges from dMRI studies on stuttering. Still, dMRI itself is a developing technique, and only recently have labs set out to investigate the neuroanatomical foundation of quantitative MRI on a histological level (Filo et al., 2019; Weiskopf, Edwards, Helms, Mohammadi, & Kirilina, 2021). Thus, there is a considerable gap between microscale histology and macroscale neuroimaging, and physiological inference from dMRI studies needs caution. Therefore, to resolve the different results, one might prefer to use advanced neuroimaging and cutting-edge methods that outperform early attempts to measure white matter microstructure. Furthermore, it would be desirable to make dMRI raw data available to enable comparative studies with established and novel analysis approaches.

In sum, additional studies are needed to derive a coherent and integrative picture because, to date, moderate sample sizes of early studies and methodological limitations of DTI fiber tracking techniques constrain the explanatory power of dMRI studies on stuttering.

5 | CONCLUSION

Here we show for the first time that white matter diffusion metrics of significant speech tracts, namely the SLF and the FAT, remain unchanged after an intensive long-term stuttering treatment with daily practice throughout 1 year. Future studies must monitor brain structure properties within shorter time intervals to capture possible transient processes that might occur earlier in fluency-shaping-related stuttering remediation. Furthermore, brain-behavior relationships indicate that the tract's composition relates to therapy outcome. This observation informs about the neurostructural basis of successful stuttering remediation.

AUTHOR CONTRIBUTIONS
All authors conceptualized and designed the study. Annika Primaßin acquired all data. Annika Primaßin and Alexandra Korzeczek analyzed the behavioral data. Nicole E. Neef analyzed the dMRI data and drafted the manuscript. All authors reviewed the manuscript.

DATA AVAILABILITY STATEMENT
All data required to support the conclusions in the paper are given in the paper and/or the Supplementary Materials. Additional data related to this paper may be obtained from the authors upon request. Only fully anonymized data can be provided. The code used in this study will be provided upon reasonable request.

ORCID
Nicole E. Neef https://orcid.org/0000-0003-2414-7595

REFERENCES
Amemiya, K., Naito, E., & Takemura, H. (2021). Age dependency and lateralization in the three branches of the human superior longitudinal fasciculus. *Cortex, 139,* 116–133.

Baboyan, V., Basilakos, A., Yourganov, G., Rorden, C., Bonilha, L., Fridriksson, J., & Hickok, G. (2021). Isolating the white matter circuitry of the dorsal language stream: Connectome-symptom mapping in stroke induced aphasia. *Human Brain Mapping, 42,* 5689–5702.

Beck, D., de Lange, A.-M. G., Maximov, I. I., Richard, G., Andreassen, O. A., Nordvik, J. E., & Westlye, L. T. (2021). White matter microstructure across the adult lifespan: A mixed longitudinal and cross-sectional study using advanced diffusion models and brain-age prediction. *NeuroImage, 224,* 117441.

Bihan, D. L., Mangin, J. F., Poupon, C., Clark, C. A., Pappata, S., Molko, N., & Chabriat, H. (2001). Diffusion tensor imaging: Concepts and applications. *Journal of Magnetic Resonance Imaging, 13,* 534–546.

Bonilha, L., Hillis, A. E., Wilmskoetter, J., Hickok, G., Basilakos, A., Munsell, B., … Fridriksson, J. (2019). Neural structures supporting spontaneous and assisted (entrained) speech fluency. *Brain, 142,* 3951–3962.

Busan, P., Ben, G. D., Russo, L. R., Bernardini, S., Natarelli, G., Arcara, G., … Battaglini, P. P. (2019). Stuttering as a matter of delay in neural activation: A combined TMS/EEG study. *Clinical Neurophysiology, 130,* 61–76.

Cai, S., Tourville, J. A., Beal, D. S., Perkell, J. S., Guenther, F. H., & Ghosh, S. S. (2014). Diffusion imaging of cerebral white matter in persons who stutter: Evidence for network-level anomalies. *Frontiers in Human Neuroscience, 8,* 54.

Catani, M., & Bambini, V. (2014). A model for social communication and language evolution and development (SCALED). *Current Opinion in Neurobiology, 28,* 165–171.

Catani, M., Dell'Acqua, F., Vergani, F., Malik, F., Hodge, H., Roy, P., … de Schotten, M. T. (2012). Short frontal lobe connections of the human brain. *Cortex, 48,* 273–291.

Catani, M., Jones, D. K., & ffytche, D. H. (2005). Perisylvian language networks of the human brain. *Annals of Neurology, 57,* 8–16.

Catani, M., & Mesulam, M. (2008). The arcuate fasciculus and the disconnection theme in language and aphasia: History and current state. *Cortex*, *44*, 953–961.

Catani, M., Mesulam, M. M., Jakobsen, E., Malik, F., Martersteck, A., Wieneke, C., ... Rogalski, E. (2013). A novel frontal pathway underlies verbal fluency in primary progressive aphasia. *Brain: A Journal of Neurology*, *136*, 2619–2628.

Chang, S.-E., Garnett, E. O., Etchell, A., & Chow, H. M. (2019). Functional and neuroanatomical bases of developmental stuttering: Current insights. *Neuroscience*, *25*, 566–582.

Chang, S.-E., & Guenther, F. H. (2020). Involvement of the Cortico-Basal Ganglia-Thalamocortical Loop in Developmental Stuttering. *Frontiers in Psychology*, *10*. https://doi.org/10.3389/fpsyg.2019.03088

Chang, S.-E., Horwitz, B., Ostuni, J., Reynolds, R., & Ludlow, C. L. (2011). Evidence of left inferior frontal–premotor structural and functional connectivity deficits in adults who stutter. *Cerebral Cortex*, *21*, 2507–2518.

Chow, H. M., & Chang, S. (2017). White matter developmental trajectories associated with persistence and recovery of childhood stuttering. *Human Brain Mapping*, *38*, 3345–3359.

Cieslak, M., Ingham, R. J., Ingham, J. C., & Grafton, S. T. (2015). Anomalous White matter morphology in adults who stutter. *Journal of Speech, Language, and Hearing Research*, *58*, 268–277.

Cler, G. J., Krishnan, S., Papp, D., Wiltshire, C. E. E., Chesters, J., & Watkins, K. E. (2021). Elevated iron concentration in putamen and cortical speech motor network in developmental stuttering. *Brain*, *144*, 2979–2984.

Connally, E. L., Ward, D., Howell, P., & Watkins, K. E. (2014). Disrupted white matter in language and motor tracts in developmental stuttering. *Brain and Language*, *131*, 25–35.

Cox, S. R., Ritchie, S. J., Tucker-Drob, E. M., Liewald, D. C., Hagenaars, S. P., Davies, G., ... Deary, I. J. (2016). Ageing and brain white matter structure in 3,513 UKbiobank participants. *Nature Communications*, *7*, 13629.

Darainy, M., Vahdat, S., & Ostry, D. J. (2019). Neural basis of sensorimotor plasticity in speech motor adaptation. *Cerebral Cortex*, *29*, 2876–2889.

de Schotten, M. T., Dell'Acqua, F., Valabregue, R., & Catani, M. (2012). Monkey to human comparative anatomy of the frontal lobe association tracts. *Cortex*, *48*, 82–96.

Dick, A. S., Garic, D., Graziano, P., & Tremblay, P. (2018). The frontal aslant tract (FAT) and its role in speech, language and executive function. *Cortex*, *111*, 148–163.

Drijkoningen, D., Caeyenberghs, K., Leunissen, I., Linden, C. V., Leemans, A., Sunaert, S., ... Swinnen, S. P. (2015). Training-induced improvements in postural control are accompanied by alterations in cerebellar white matter in brain injured patients. *Neuroimage: Clinical*, *7*, 240–251.

Eggers, K., Nil, L. F. D., & van den Bergh, B. R. (2013). Inhibitory control in childhood stuttering. *Journal of Fluency Disorders*, *38*, 1–13.

Eickhoff, S. B., Bzdok, D., Laird, A. R., Roski, C., Caspers, S., Zilles, K., & Fox, P. T. (2011). Co-activation patterns distinguish cortical modules, their connectivity and functional differentiation. *NeuroImage*, *57*, 938–949.

Elmer, S., Hänggi, J., Vaquero, L., Cadena, G. O., François, C., & Rodríguez-Fornells, A. (2019). Tracking the microstructural properties of the main white matter pathways underlying speech processing in simultaneous interpreters. *NeuroImage*, *191*, 518–528.

Erika-Florence, M., Leech, R., & Hampshire, A. (2014). A functional network perspective on response inhibition and attentional control. *Nature Communications*, *5*, 4073.

Euler, H. A., Merkel, A., Hente, K., Neef, N., von Gudenberg, A. W., & Neumann, K. (2021). Speech restructuring group treatment for 6-to-9-year-old children who stutter: A therapeutic trial. *Journal of Communication Disorders*, *89*, 106073.

Euler, H. A., von Gudenberg, A. W., Jung, K., & Neumann, K. (2009). Computergestützte Therapie bei Redeflussstörungen: Die langfristige Wirksamkeit der Kasseler Stottertherapie (KST). *Sprache Stimme Gehor*, *33*, 193–202.

Filo, S., Shtangel, O., Salamon, N., Kol, A., Weisinger, B., Shifman, S., & Mezer, A. A. (2019). Disentangling molecular alterations from water-content changes in the aging human brain using quantitative MRI. *Nature Communications*, *10*, 3403.

Finkl, T., Hahne, A., Friederici, A. D., Gerber, J., Mürbe, D., & Anwander, A. (2019). Language without speech: Segregating distinct circuits in the human brain. *Cerebral Cortex*, *30*(2), 812–823.

Freud, D., & Amir, O. (2020). Resilience in people who stutter: Association with covert and overt characteristics of stuttering. *Journal of Fluency Disorders*, *64*, 105761.

Friederici, A. D., Bahlmann, J., Heim, S., Schubotz, R. I., & Anwander, A. (2006). The brain differentiates human and non-human grammars: Functional localization and structural connectivity. *Proceedings of the National Academy of Sciences of the United States of America*, *103*, 2458–2463.

Frigerio-Domingues, C. E., Gkalitsiou, Z., Zezinka, A., Sainz, E., Gutierrez, J., Byrd, C., ... Drayna, D. (2019). Genetic factors and therapy outcomes in persistent developmental stuttering. *Journal of Communication Disorders*, *80*, 11–17.

Gallardo, G., Wassermann, D., & Anwander, A. (2020). Bridging the gap: From neuroanatomical knowledge to Tractography of brain pathways. *Biorxiv*, *2020*, 232116.

Garic, D., Broce, I., Graziano, P., Mattfeld, A., & Dick, A. S. (2019). Laterality of the frontal aslant tract (FAT) explains externalizing behaviors through its association with executive function. *Developmental Science*, *22*, e12744.

Garnett, E. O., Chow, H. M., Nieto-Castañón, A., Tourville, J. A., Guenther, F. H., & Chang, S.-E. (2018). Anomalous morphology in left hemisphere motor and premotor cortex of children who stutter. *Brain*, *141*, 2670–2684.

Garyfallidis, E., Brett, M., Amirbekian, B., Rokem, A., van der Walt, S., Descoteaux, M., & Nimmo-Smith, I. (2014). Dipy, a library for the analysis of diffusion MRI data. *Frontiers in Neuroinformatics*, *8*, 8. https://doi.org/10.3389/fninf.2014.00008

Giraud, A.-L., Neumann, K., Bachoud-Levi, A.-C., von Gudenberg, A. W., Euler, H. A., Lanfermann, H., & Preibisch, C. (2008). Severity of dysfluency correlates with basal ganglia activity in persistent developmental stuttering. *Brain and Language*, *104*, 190–199.

Glasser, M. F., & Rilling, J. K. (2008). DTI Tractography of the human Brain's language pathways. *Cerebral Cortex*, *18*, 2471–2482.

Guenther, F. H., & Hickok, G. (2015). Chapter 9 role of the auditory system in speech production. *Handbook of Clinical Neurology*, *129*, 161–175.

Halai, A. D., Woollams, A. M., & Ralph, M. A. L. (2017). Using principal component analysis to capture individual differences within a unified neuropsychological model of chronic post-stroke aphasia: Revealing the unique neural correlates of speech fluency, phonology and semantics. *Cortex*, *86*, 275–289.

Hallett, M., Iorio, R. D., Rossini, P. M., Park, J. E., Chen, R., Celnik, P., ... Ugawa, Y. (2017). Contribution of transcranial magnetic stimulation to assessment of brain connectivity and networks. *Clinical Neurophysiology*, *128*, 2125–2139.

Hannah, R., & Aron, A. R. (2021). Towards real-world generalizability of a circuit for action-stopping. *Nature Reviews. Neuroscience*, *22*, 538–552.

Hartwigsen, G., Neef, N. E., Camilleri, J. A., Margulies, D. S., & Eickhoff, S. B. (2019). Functional segregation of the right inferior frontal gyrus: Evidence from Coactivation-based Parcellation. *Cerebral Cortex*, *29*, 1532–1546.

Hickok, G., Houde, J., & Rong, F. (2011). Sensorimotor integration in speech processing: Computational basis and neural organization. *Neuron*, *69*, 407–422.

Hickok, G., & Poeppel, D. (2007). The cortical organization of speech processing. *Nature Reviews. Neuroscience*, *8*, 393–402.

Huber, E., Donnelly, P. M., Rokem, A., & Yeatman, J. D. (2018). Rapid and widespread white matter plasticity during an intensive reading intervention. *Nature Communications*, 9, 2260.

Jäncke, L., Hänggi, J., & Steinmetz, H. (2004). Morphological brain differences between adult stutterers and non-stutterers. *BMC Neurology*, 4, 23.

Johnson, C., Liu, Y., Waller, N., & Chang, S.-E. (in press). Tract profiles of the cerebellar peduncles in children who stutter. *Brain Structure & Function*. https://doi.org/10.1007/s00429-022-02471-4

Jones, D. K., Knösche, T. R., & Turner, R. (2013). White matter integrity, fiber count, and other fallacies: The do's and don'ts of diffusion MRI. *NeuroImage*, 73, 239–254. https://doi.org/10.1016/j.neuroimage.2012.06.081

Jossinger, S., Kronfeld-Duenias, V., Zislis, A., Amir, O., & Ben-Shachar, M. (2021). Speech rate association with cerebellar white-matter diffusivity in adults with persistent developmental stuttering. *Brain Structure & Function*, 226, 801–816.

Jossinger, S., Sares, A., Zislis, A., Suri-Barot, D., Gracco, V., & Ben-Shachar, M. (2021). White matter correlates of sensorimotor synchronization in persistent developmental stuttering. *Journal of Communication Disorders*, 95, 106169.

Kell, C. A., Neumann, K., Behrens, M., von Gudenberg, A. W., & Giraud, A.-L. (2018). Speaking-related changes in cortical functional connectivity associated with assisted and spontaneous recovery from developmental stuttering. *Journal of Fluency Disorders*, 55, 135–144.

Kell, C. A., Neumann, K., von Kriegstein, K., Posenenske, C., von Gudenberg, A. W., Euler, H., & Giraud, A.-L. (2009). How the brain repairs stuttering. *Brain*, 132, 2747–2760.

Kemerdere, R., de Champfleur, N. M., Deverdun, J., Cochereau, J., Moritz-Gasser, S., Herbet, G., & Duffau, H. (2016). Role of the left frontal aslant tract in stuttering: A brain stimulation and tractographic study. *Journal of Neurology*, 263, 157–167.

Kim, K. S., & Max, L. (2021). Speech auditory-motor adaptation to formant-shifted feedback lacks an explicit component: Reduced adaptation in adults who stutter reflects limitations in implicit sensorimotor learning. *The European Journal of Neuroscience*, 53, 3093–3108.

Koenraads, S. P. C., van der Schroeff, M. P., van Ingen, G., Lamballais, S., Tiemeier, H., de RJB, J., ... Muetzel, R. L. (2020). Structural brain differences in pre-adolescents who persist in and recover from stuttering. *Neuroimage: Clinical*, 27, 102334.

Korzeczek, A., Primaßin, A., von Gudenberg, A. W., Dechent, P., Paulus, W., Sommer, M., & Neef, N. E. (2021). Fluency shaping increases integration of the command-to-execution and the auditory-to-motor pathways in persistent developmental stuttering. *NeuroImage*, 245, 118736.

Kronfeld-Duenias, V., Amir, O., Ezrati-Vinacour, R., Civier, O., & Ben-Shachar, M. (2016a). Dorsal and ventral language pathways in persistent developmental stuttering. *Cortex*, 81, 79–92.

Kronfeld-Duenias, V., Amir, O., Ezrati-Vinacour, R., Civier, O., & Ben-Shachar, M. (2016b). The frontal aslant tract underlies speech fluency in persistent developmental stuttering. *Brain Structure & Function*, 221, 365–381.

Kronfeld-Duenias, V., Civier, O., Amir, O., Ezrati-Vinacour, R., & Ben-Shachar, M. (2018). White matter pathways in persistent developmental stuttering: Lessons from tractography. *Journal of Fluency Disorders*, 55, 68–83.

Landers, M. J. F., Meesters, S. P. L., van Zandvoort, M., de Baene, W., & Rutten, G.-Jan M. (in press). The frontal aslant tract and its role in executive functions: a quantitative tractography study in glioma patients. *Brain Imaging and Behavior*. https://doi.org/10.1007/s11682-021-00581-x

Lebel, C., Gee, M., Camicioli, R., Wieler, M., Martin, W., & Beaulieu, C. (2012). Diffusion tensor imaging of white matter tract evolution over the lifespan. *NeuroImage*, 60, 340–352.

Lehmann, N., Villringer, A., & Taubert, M. (2020). Colocalized White matter plasticity and increased cerebral blood flow mediate the beneficial effect of cardiovascular exercise on Long-term motor learning. *The Journal of Neuroscience*, 40, 2416–2429.

Lu, C., Chen, C., Peng, D., You, W., Zhang, X., Ding, G., ... Howell, P. (2012). Neural anomaly and reorganization in speakers who stutter. *Neurology*, 79, 625–632.

Lu, C., Zheng, L., Long, Y., Yan, Q., Ding, G., Liu, L., ... Howell, P. (2017). Reorganization of brain function after a short-term behavioral intervention for stuttering. *Brain and Language*, 168, 12–22.

Madhyastha, T., Mérillat, S., Hirsiger, S., Bezzola, L., Liem, F., Grabowski, T., & Jäncke, L. (2014). Longitudinal reliability of tract-based spatial statistics in diffusion tensor imaging. *Human Brain Mapping*, 35, 4544–4555.

Maeda, Y., Kim, H., Kettner, N., Kim, J., Cina, S., Malatesta, C., ... Napadow, V. (2017). Rewiring the primary somatosensory cortex in carpal tunnel syndrome with acupuncture. *Brain*, 140, 914–927.

Markett, S., Bleek, B., Reuter, M., Prüss, H., Richardt, K., Müller, T., ... Montag, C. (2016). Impaired motor inhibition in adults who stutter—Evidence from speech-free stop-signal reaction time tasks. *Neuropsychologia*, 91, 444–450.

Matias-Guiu, J. A., Suárez-Coalla, P., Yus, M., Pytel, V., Hernández-Lorenzo, L., Delgado-Alonso, C., ... Cuetos, F. (2022). Identification of the main components of spontaneous speech in primary progressive aphasia and their neural underpinnings using multimodal MRI and FDG-PET imaging. *Cortex*, 146, 141–160.

Max, L., & Caruso, A. J. (1997). Contemporary techniques for establishing fluency in the treatment of adults who stutter. *Contemporary Issues in Communication Science and Disorders*, 24, 39–46.

Mazerolle, E. L., Warwaruk-Rogers, R., Romo, P., Sankar, T., Scott, S., Rockel, C. P., ... Pike, G. B. (2021). Diffusion imaging changes in the treated tract following focused ultrasound thalamotomy for tremor. *Neuroimage: Reports*, 1, 100010. https://doi.org/10.1016/j.ynirp.2021.100010

Metzger, F. L., Auer, T., Helms, G., Paulus, W., Frahm, J., Sommer, M., & Neef, N. E. (2018). Shifted dynamic interactions between subcortical nuclei and inferior frontal gyri during response preparation in persistent developmental stuttering. *Brain Structure & Function*, 223, 165–182.

Metzler-Baddeley, C., Foley, S., de Santis, S., Charron, C., Hampshire, A., Caeyenberghs, K., & Jones, D. K. (2017). Dynamics of White matter plasticity underlying working memory training: Multimodal evidence from diffusion MRI and Relaxometry. *Journal of Cognitive Neuroscience*, 29, 1509–1520.

Misaghi, E., Zhang, Z., Gracco, V. L., Nil, L. F. D., & Beal, D. S. (2018). White matter tractography of the neural network for speech-motor control in children who stutter. *Neuroscience Letters*, 668, 37–42.

Miyake, A., & Friedman, N. P. (2012). The nature and Organization of Individual Differences in executive functions: Four general conclusions. *Current Directions in Psychological Science*, 21, 8–14.

Neef, N. E., Anwander, A., Bütfering, C., Schmidt-Samoa, C., Friederici, A. D., Paulus, W., & Sommer, M. (2017). Structural connectivity of right frontal hyperactive areas scales with stuttering severity. *Brain*, 141, 191–204.

Neef, N. E., Anwander, A., & Friederici, A. D. (2015). The neurobiological grounding of persistent stuttering: From structure to function. *Current Neurology and Neuroscience Reports*, 15, 63.

Neef, N. E., Bütfering, C., Anwander, A., Friederici, A. D., Paulus, W., & Sommer, M. (2016). Left posterior-dorsal area 44 couples with parietal areas to promote speech fluency, while right area 44 activity promotes the stopping of motor responses. *NeuroImage*, 142, 628–644.

Neef, N. E., Primaßin, A., von Gudenberg, A. W., Dechent, P., Riedel, H. C., Paulus, W., & Sommer, M. (2021). Two cortical representations of voice control are differentially involved in speech fluency. *Brain Communications*, 3, fcaa232.

Neumann, K., Euler, H. A., Kob, M., von Gudenberg, A. W., Giraud, A.-L., Weissgerber, T., & Kell, C. A. (2018). Assisted and unassisted recession of functional anomalies associated with dysprosody in adults who stutter. *Journal of Fluency Disorders*, 55, 120–134.

Nil, L. F. D., Kroll, R. M., & Houle, S. (2001). Functional neuroimaging of cerebellar activation during single word reading and verb generation in stuttering and nonstuttering adults. *Neuroscience Letters*, *302*, 77–80.

Perron, M., Theaud, G., Descoteaux, M., & Tremblay, P. (2021). The frontotemporal organization of the arcuate fasciculus and its relationship with speech perception in young and older amateur singers and non-singers. *Human Brain Mapping*, *42*, 3058–3076.

Primaßin, A. (2019). Longitudinal structural and functional brain changes associated with stuttering improvement by therapy or brain lesion (PhD Thesis), Göttingen University.

Quallo, M. M., Price, C. J., Ueno, K., Asamizuya, T., Cheng, K., Lemon, R. N., & Iriki, A. (2009). Gray and white matter changes associated with tool-use learning in macaque monkeys. *Proceedings of the National Academy of Sciences of the United States of America*, *106*, 18379–18384.

Reed, A., Cummine, J., Bakhtiari, R., Fox, C. M., & Boliek, C. A. (2017). Changes in White matter integrity following intensive voice treatment (LSVT LOUD®) in children with cerebral palsy and motor speech disorders. *Developmental Neuroscience*, *39*, 460–471.

Reid, L. B., Sale, M. V., Cunnington, R., Mattingley, J. B., & Rose, S. E. (2017). Brain changes following four weeks of unimanual motor training: Evidence from fMRI-guided diffusion MRI tractography. *Human Brain Mapping*, *38*, 4302–4312.

Riley, G. D. (2009). *SSI-4: Stuttering severity instrument* (4th ed.). Torrance, CA: WPS Publishing.

Rutten, G.-J. M., Landers, M. J. F., Baene, W. D., Meijerink, T., van der Hek, S., & Verheul, J. H. B. (2021). Executive functional deficits during electrical stimulation of the right frontal aslant tract. *Brain Imaging and Behavior*, *15*, 2731–2735.

Sarubbo, S., Benedictis, A. D., Merler, S., Mandonnet, E., Balbi, S., Granieri, E., & Duffau, H. (2015). Towards a functional atlas of human white matter. *Human Brain Mapping*, *36*, 3117–3136.

Saur, D., Kreher, B. W., Schnell, S., Kümmerer, D., Kellmeyer, P., Vry, M.-S., … Weiller, C. (2008). Ventral and dorsal pathways for language. *Proceedings of the National Academy of Sciences of the United States of America*, *105*, 18035–18040.

Schmahmann, J. D., & Pandya, D. N. (2006). Superior temporal region. In *Fiber pathways of the brain* (pp. 143–186). New York, NY: Oxford University Press.

Scholz, J., Klein, M. C., Behrens, T. E. J., & Johansen-Berg, H. (2009). Training induces changes in white-matter architecture. *Nature Neuroscience*, *12*, 1370–1371.

Song, S.-K., Yoshino, J., Le, T. Q., Lin, S.-J., Sun, S.-W., Cross, A. H., & Armstrong, R. C. (2005). Demyelination increases radial diffusivity in corpus callosum of mouse brain. *NeuroImage*, *26*, 132–140.

Sullivan, E. V., & Pfefferbaum, A. (2006). Diffusion tensor imaging and aging. *Neuroscience and Biobehavioral Reviews*, *30*, 749–761.

Taubert, M., Draganski, B., Anwander, A., Müller, K., Horstmann, A., Villringer, A., & Ragert, P. (2010). Dynamic properties of human brain structure: Learning-related changes in cortical areas and associated fiber connections. *The Journal of Neuroscience*, *30*, 11670–11677.

Taubert, M., Villringer, A., & Ragert, P. (2012). Learning-related gray and White matter changes in humans. *Neuroscience*, *18*, 320–325.

Toyomura, A., Fujii, T., & Kuriki, S. (2015). Effect of an 8-week practice of externally triggered speech on basal ganglia activity of stuttering and fluent speakers. *NeuroImage*, *109*, 458–468.

Treleaven, S. B., & Coalson, G. A. (2020). Manual response inhibition and quality of life in adults who stutter. *Journal of Communication Disorders*, *88*, 106053.

Tseng, W.-Y. I., Hsu, Y.-C., Chen, C.-L., Kang, Y.-J., Kao, T.-W., Chen, P.-Y., & Waiter, G. D. (2021). Microstructural differences in white matter tracts across middle to late adulthood: A diffusion MRI study on 7167 UKbiobank participants. *Neurobiology of Aging*, *98*, 160–172.

Voineskos, A. N., Rajji, T. K., Lobaugh, N. J., Miranda, D., Shenton, M. E., Kennedy, J. L., … Mulsant, B. H. (2012). Age-related decline in white matter tract integrity and cognitive performance: A DTI tractography and structural equation modeling study. *Neurobiology of Aging*, *33*, 21–34.

von Gudenberg, A. W., & Euler, H. A. (2000). Evaluation study of the Kasseler stuttering therapy (KST). *Journal of Fluency Disorders*, *25*, 195.

Wan, C. Y., Zheng, X., Marchina, S., Norton, A., & Schlaug, G. (2014). Intensive therapy induces contralateral white matter changes in chronic stroke patients with Broca's aphasia. *Brain and Language*, *136*, 1–7.

Warrington, S., Bryant, K. L., Khrapitchev, A. A., Sallet, J., Charquero-Ballester, M., Douaud, G., … Sotiropoulos, S. N. (2020). XTRACT—Standardised protocols for automated tractography in the human and macaque brain. *NeuroImage*, *217*, 116923.

Watkins, K. E., Chesters, J., & Connally, E. L. (2016). The neurobiology of developmental stuttering. In G. Hickok & S. Small (Eds.), *Neurobiology of language* (pp. 995–1004). Cambridge, MA: MIT Press.

Watkins, K. E., Smith, S. M., Davis, S., & Howell, P. (2008). Structural and functional abnormalities of the motor system in developmental stuttering. *Brain*, *131*, 50–59.

Webster, R. L. (1974). A behavioral analysis of stuttering: Treatment and theory. In K. S. Calhoun, H. E. Adams, & K. M. Mitchell (Eds.), *Innovative treatment methods in psychopathology*. New York, NY: Wiley.

Webster, R. L. (1980). *The precision fluency shaping program: Speech Reconstruction for Stutterers*. Roanoke, VA: Communications Development Corporation.

Weiskopf, N., Edwards, L. J., Helms, G., Mohammadi, S., & Kirilina, E. (2021). Quantitative magnetic resonance imaging of brain anatomy and in vivo histology. *Nature Reviews Physics*, *3*, 570–588.

Yaruss, J. S., & Quesal, R. W. (2006). Overall assessment of the speaker's experience of stuttering (OASES): Documenting multiple outcomes in stuttering treatment. *Journal of Fluency Disorders*, *31*, 90–115.

Yaruss, J. S., & Quesal, R. W. (2014). *OASES: Overall assessment of the speaker's experience of stuttering [Trans. Deutsche Übersetzung: H. A. Euler, & A. Alpermann]*. Bloomington, IN: Pearson Assessments.

Yeatman, J. D., Dougherty, R. F., Myall, N. J., Wandell, B. A., & Feldman, H. M. (2012). Tract profiles of White matter properties: Automating fiber-tract quantification. *PLoS One*, *7*, e49790.

Yeatman, J. D., Wandell, B. A., & Mezer, A. A. (2014). Lifespan maturation and degeneration of human brain white matter. *Nature Communications*, *5*, 4932.

Zatorre, R. J., Fields, R. D., & Johansen-Berg, H. (2012). Plasticity in gray and white: Neuroimaging changes in brain structure during learning. *Nature Neuroscience*, *15*, 528–536.

SUPPORTING INFORMATION

Additional supporting information may be found in the online version of the article at the publisher's website.